p38 signaling enhances short-lived effector cell differentiation and weakens central memory CD8+ T-cell formation

Lichen Hu, Huaipeng Lin, Yubing Fu, Danying Li, Yu Cong, Wanyun Li, Zexu Wang, Lei Zhang, Guo Fu, Nengming Xiao, Jiahuai Han, Jianfeng Wu

The Journal of Immunology, 2025, **00**, 1–17
https://doi.org/10.1093/jimmun/vkaf214
Research Article

p38 signaling enhances short-lived effector cell differentiation and weakens central memory CD8$^+$ T-cell formation

Lichen Hu[1], Huaipeng Lin[1], Yubing Fu[1], Danying Li[1], Yu Cong[1], Wanyun Li[1], Zexu Wang[1], Lei Zhang[1], Guo Fu[1], Nengming Xiao[1], Jiahuai Han[1,2,*], and Jianfeng Wu[1,3,*]

[1]State Key Laboratory of Cellular Stress Biology, School of Life Sciences, Faculty of Medicine and Life Sciences, Xiamen University, Xiamen, China
[2]Research Unit of Cellular Stress of Chinese Academy of Medical Sciences, Xiang'an Hospital of Xiamen University, Cancer Research Center of Xiamen University, School of Medicine, Faculty of Medicine and Life Sciences, Xiamen University, Xiamen, China
[3]Laboratory Animal Center, Faculty of Medicine and Life Sciences, Xiamen University, Xiamen, China

*Address correspondence and reprint requests to Dr. Jianfeng Wu or Dr. Jiahuai Han, State Key Laboratory of Cellular Stress Biology, School of Life Sciences, Xiamen University, Xiang'an Campus, Xiang'an District, Xiamen 361102, China. Email: wzqwjf0728@xmu.edu.cn (J.F.W.) or jhan@xmu.edu.cn (J.H.)

Abstract

Memory CD8$^+$ T cells are essential for long-term protective immunity. Here, we show that activation of p38 MAPK during the primary response of CD8$^+$ T cells orchestrates a delicate balance between the formation of short-lived effector cells and memory precursor effector cells. *p38α*$^{fl/fl}$*p38β*$^{fl/fl}$*GzmB*$^{cre/-}$ mice, in which *p38α* and *p38β* were efficiently deleted in CD8$^+$ T cells and also in early stages of T-cell development, were used in studying the role of the p38 pathway in T cells. The deletion of *p38α* and *p38β* (simplified as *p38α/β*) has very minor effects on thymic and peripheral T-cell development. In contrast, *p38α/β*-deficient CD8$^+$ T cells were skewed toward a central memory phenotype and mounted stronger recall responses upon secondary challenge. Transcriptomic analyses of antigen-specific CD8$^+$ T cells revealed that *p38α/β* deficiency is associated with reduced effector gene expression and enhanced memory-associated programs. Furthermore, in vitro differentiated *p38α/β*-deficient CD8$^+$ T cells showed superior persistence and functional responses after adoptive transfer. These results establish a role for p38 in controlling effector CD8$^+$ T-cell differentiation and memory formation, and reinforce the therapeutic potential of targeting this pathway, aligning with recent studies demonstrating the beneficial effects of p38 inhibitors in adoptive cell therapy.

Keywords: p38, CD8$^+$ T cell, LCMV, cell differentiation, memory

Introduction

CD8$^+$ T cells are vital components of the adaptive immune system, characterized by their immune memory signature and their ability to confer specific protective immunity against infected or tumor cells.[1] The activation of CD8$^+$ T cells occurs through the reception of T-cell receptor (TCR) and co-stimulatory signals from antigen-presenting cells (APCs). Upon activation, these cells undergo continuous division, giving rise to effector populations that work to eliminate pathogenic invaders.[2] Effector CD8$^+$ T cells directly kill the target cells through various mechanisms, including the expression of FasL, secretion of toxic molecules such as granzymes and perforin, and release of inflammatory cytokines like IFN-γ and TNF-α.[3] Following pathogen clearance, the majority of effector T cells undergo apoptosis, while a small proportion transition into a memory phase over time.[2] The cytolytic function of CD8$^+$ T cells also designates them as cytotoxic T lymphocytes (CTLs), the integral executor of cellular immunity.[1] Effector CD8$^+$ T-cell responses to infection typically manifest as heterogeneous populations due to the complexity of the microenvironment.[2,4] Among these populations, 2 distinct subsets emerge: short-lived effector cells (SLECs), identified by high surface expression of KLRG1 and low expression of CD127 (KLRG1^{hi}CD127^{lo}), and oppositely marked cell population (KLRG1^{lo}CD127^{hi}), named memory precursor effector cells (MPECs).[5] MPECs demonstrate an enhanced potential to differentiate into long-lasting memory CD8$^+$ T cells.[6]

Memory CD8$^+$ T cells play a role as a crucial component of immune memory, rapidly mobilizing effector responses upon reinfection and providing long-term defense against previously encountered threats.[1] These memory CD8$^+$ T cells can be classified into effector memory (Tem), central memory (Tcm), and tissue-resident memory T cells.[7] Among them, Tcm is extremely capable of producing IL-2, which boosts T-cell division in a paracrine or autocrine manner.[8–10] Tcm cells accumulate slowly in secondary lymphoid tissues over time, expressing large amounts of CD62L, CD27, and CXCR3, whereas Tem cells lack expression of lymphocyte homing receptor CD62L and circulate in the periphery.[5] The effector-to-memory CD8$^+$ T-cell transition is pivotal as it directly influences the immune efficacy.[7]

The p38 family represents a group of evolutionarily conserved mitogen-activated protein kinases (MAPKs), comprising four homologues in mammalian cells: α, β, γ, and δ.[11] Typically, p38 is activated through phosphorylation at residues Thr180 and Tyr182 in a classical Thr-X-Tyr motif via a

Received: July 3, 2024. **Accepted:** August 1, 2025

canonical pathway catalyzed by MKK3 and MKK6.[11] However, in T cells, p38α and p38β can also be activated by TCR signaling through an alternative mechanism.[12] Upon TCR ligation, the proximal tyrosine kinase ZAP70 initiates phosphorylation of p38 at the Tyr323 residue, leading to subsequent autophosphorylation of the classical motif.[13] This alternative activation mechanism of p38α is necessary for normal IFN-γ production in T cells.[14]

Several studies have addressed the role of p38 MAPKs in T-lymphocyte development and differentiation, including $CD8^+$ T cells.[15] Specifically, T cell–specific *p38α*-knockout mice exhibit lower numbers of $CD8^+$ T cells in peripheral lymphoid tissues compared to wild-type (WT) mice.[16,17] Additionally, *p38γ* knockout promotes thymocyte-positive selection from double-positive to single-positive cells, while *p38δ* knockout affects double-negative thymocyte development at various stages.[18] The concurrent deficiency of *p38α* and *p38β* leads to increased regulatory T-cell induction under specific culture conditions in $CD4^+$ T cells.[16,19] Moreover, both p38α and p38β play essential roles in regulating TCR-induced IFN-γ and TNF-α production to maintain normal Th1 effector function, with p38α being particularly crucial for cytokine-induced IFN-γ production.[20] Deletion of *p38α* reduces IFN-γ and TNF-α production in $CD8^+$ T cells activated with anti-CD3 and anti-CD28 antibodies.[19]

While p38 signaling plays a role in $CD8^+$ T-cell development, its exact in vivo function in $CD8^+$ T-cell responses remains poorly understood. Recent research employing a multiphenotype screen for effective antitumor $CD8^+$ T cells has identified p38α in $CD8^+$ T cells as a central regulator of cell expansion, CD62L expression, oxidative stress, and genomic stress,[21] and inhibition of p38 ex vivo has demonstrated significant benefits in improving the efficacy of TCR and chimeric antigen receptor T-cell therapies.[21,22] Notably, mature T cells express both p38α and p38β proteins, both of which are direct targets of most p38 inhibitors.[16] These findings highlight the importance of elucidating the in vivo function of p38 signaling in $CD8^+$ T-cell responses.

To study the function of p38 in $CD8^+$ T cells, we generated double deficiency in *p38α* and *p38β* using granzyme B–Cre (*GzmB-Cre*) mice, and investigated the role of p38α and p38β in $CD8^+$ T cells upon infection with lymphocytic choriomeningitis virus Armstrong strain ($LCMV_{Arm}$).[23,24] Although *GzmB-Cre* is designed to mediate deletion in activated $CD8^+$ T cells,[23] we observed leaky Cre activity leading to premature deletion of *p38α/β* under homeostatic conditions. Despite this early deletion, thymic development was largely intact, and total T-cell numbers were comparable between WT and conditional knockout mice, though there was a modest shift in the $CD4^+/CD8^+$ T-cell ratio. Mice with *p38α/β* deficiency in $CD8^+$ T cells exhibited partial reduction in virus-specific SLEC generation and increased accumulation of MPECs and Tcm cells compared to their WT littermates. Consistently, these mutant mice showed a stronger secondary $CD8^+$ T-cell response compared to WT mice. Interestingly, *p38α/β* deletion reduced IFN-γ and TNF-α expression levels in both effector and memory $CD8^+$ T cells in vivo but enhanced the protective capacity of in vitro differentiated $CD8^+$ T cells through prolonged engraftment persistence. We also showed that the *p38* deletion caused alterations in the expression of genes associated with T-cell activation and differentiation. These findings reveal a predominantly cell-intrinsic role for p38 MAPKs in promoting $CD8^+$ T-cell terminal differentiation. Loss of *p38α/β* appears to shift cells toward a less differentiated state during the effector phase, thereby favoring the formation of memory cells with enhanced recall potential.

Materials and methods

Mice

Mice harboring floxed *p38α* ($p38\alpha^{fl/fl}$) or floxed *p38β* ($p38\beta^{fl/fl}$) alleles were previously described.[25] $GzmB^{cre/-}$ (Jax, 003734), WT C57BL/6J (Jax, 000664), *CD45.1* B6.SJL (Jax, 002014), *Thy1.1* (Jax, 000406), and P14 (Jax, 004694) mice were originally from the Jackson Laboratory. $p38\alpha^{fl/fl}$ mice, $p38\beta^{fl/fl}$ mice, and $GzmB^{cre}$ mice were crossed to obtain $p38\alpha^{fl/fl}p38\beta^{fl/fl}GzmB^{cre/-}$ mice. $p38\alpha^{fl/fl}p38\beta^{fl/fl}GzmB^{cre/-}$ mice were further bred with P14 mice for the isolation of LCMV D^b-GP_{33-41}-specific $CD8^+$ T cells. All mice were backcrossed to the C57BL/6J background at least 6 generations and maintained under specific pathogen–free conditions on a 12-hour light-dark cycle (lights on 8 a.m. to 8 p.m.) at the Laboratory Animal Center of Xiamen University. The room humidity was 50% to 70%, and the room temperature was 22 °C to 24 °C. All the animal experiments were conducted according to the guidelines of the Animal Care and Use Committee of Xiamen University (XMULAC20210073).

Antibodies and reagents

Antibodies and reagents used in this research are listed in Table S1 in the Supplementary material.

Infection models

For the primary LCMV infection model and recall response of adoptively transferred $CD8^+$ T cells, mice were infected intraperitoneally (i.p.) with 2×10^5 PFU of $LCMV_{Arm}$.

For the secondary immune response assay, mice were first infected i.p. with $LCMV_{Arm}$; over 60 days later, mice were rechallenged i.p. with 5×10^4 CFU of *Listeria monocytogenes* expressing the LCMV epitope GP_{33-41} (Lm-gp33), and responses were analyzed at day 7 after infection.

To evaluate the function of in vitro differentiated $CD8^+$ T cells, 2×10^5 cultured cells were transferred to WT mice, and the mice were then intravenously (i.v.) infected with 2×10^6 focus-forming unit (FFU) of LCMV Clone 13 ($LCMV_{Cl13}$) the next day. Serum viral titers were measured 10 days later after infection using a focus-forming assay on Vero cells.

Lymphocyte isolation and Western blotting

To isolate tissue infiltrating lymphocytes, liver and lung were cut into pieces and digested with Collagenase Type IV. The turbid samples were then grinded and filtered through a 70-μm strainer mesh, and lymphocytes were separated by discontinuous Percoll density gradient centrifugation (42% and 70%). Cells were counted using Countstar analyzer (IC1000). For Western blotting, splenic $CD8^+$ T cells were purified from uninfected or infected mice at indicated time points, and the protein levels of p38 and phosphorylated p38 (p-p38) in purified splenic $CD8^+$ T cells were detected as previously described.[25] The intensity was calculated with ImageJ software (v1.4.3.67).

Flow cytometry

Single-cell suspensions were prepared from thymus, spleen, lymph node, liver, lung, or blood of mice. MHC-I D^b-GP_{33-41} tetramer was used to identify antigen-specific $CD8^+$ T cells.[26] For intracellular staining, cells were initially incubated with surface antibodies, fixed, and permeabilized, followed by cytoplasmic antibody incubation according to the manufacturer's instructions (BD Biosciences, 554722). For determining cytokine expression, cells were stimulated with 1 μg/mL GP_{33-41} or $NP_{396-404}$ peptide in RPMI 1640 medium for 5 hours at 37 °C in the presence of Brefeldin A prior to staining. For viability detection, Annexin V and 7-AAD staining was performed in binding buffer. Sample information was collected on a Fortessa X-20 (BD Biosciences) and analyzed with FlowJo software (Tree Star, v10).

Mass cytometry (time-of-flight mass cytometry)

In brief, splenocytes from $LCMV_{Arm}$-infected $p38\alpha^{fl/fl}p38\beta^{fl/fl}$ and $p38\alpha^{fl/fl}p38\beta^{fl/fl}GzmB^{cre/-}$ mice at day 8 were prepared. Cells were then labeled with rhodium (Fluidigm) for viability and blocked with anti-mouse CD16/32 followed by staining with metal-conjugated antibodies. The marker panel of antibodies is indicated in Fig. 2C and DNA content was concerned to select intact single cells. Sample information was acquired on CyTOF2 equipment (Fluidigm) and data were normalized using the Helios 6.5.358 acquisition software (Fluidigm). The data were further unpacked using the cytofkit and cytofexplorer package (http://github.com/XinleiChen001/cytofexplorer) in R software. After extracting the expression values of all cells for these 30 markers and transformation, 5,000 cells were sampled from each flow cytometry standard (FCS) file using the *ceil* method and then combined into one expression matrix. Clustering analysis was performed using the PhenoGraph method to implement subset detection. Then t-distributed stochastic neighbor embedding (t-SNE) dimensionality reduction method was integrated to visualize the high-dimensional mass cytometry data, with point color representing the cell type detected from cluster analysis. A heatmap was generated based on the median expression level of each marker in each cell type, and specified marker expression patterns on the dimensionality-reduced map were visualized by colors representing values. The percentage of cells in each cluster for each FCS file was tabulated for subset abundance comparison.

In vivo antigen-specific killing assay[27]

Splenocytes from CD45.1 mice were pulsed with or without 0.2 ng/mL GP_{33-41} peptide in RPMI 1640 medium at 37 °C for 1 hour. The peptide-pulsed cells were then incubated with the lower concentration of CFSE (0.5 μM), while the unpulsed cells were incubated with a higher concentration of CFSE (5 μM). Peptide-pulsed target cells and unpulsed control cells were further mixed at a 1:1 ratio, and a total of 2×10^7 mixed cells was transferred i.v. to the previously infected mice. Four hours later, the proportions of splenic $CFSE^{lo}$ peptide-pulsed cells in transferred cells were determined and calculated to represent antigen-specific killing ability.

In vitro killing experiment

Following the recall response, splenic D^b-GP_{33-41}-$tetramer^+$ $CD8^+$ T cells were sorted from $p38\alpha^{fl/fl}p38\beta^{fl/fl}$ and $p38\alpha^{fl/fl}p38\beta^{fl/fl}GzmB^{cre/-}$ mice. EL4 target cells were labeled with 2 μM PKH67 and treated with 15 μg/mL Mitomycin C for 30 minutes, and then incubated with 2 μg/mL GP_{33-41} peptide for 1 hour at a density of 1×10^7 cells/mL. Purified $CD8^+$ T cells were mixed with peptide-loaded EL4 cells at various effector-to-target ratios; 8 hours later, killing activity was assessed by propidium iodide staining.

Adoptive transfer experiments

For adoptive transfer, splenic naïve $CD8^+$ T cells were purified. $p38\alpha^{fl/fl}p38\beta^{fl/fl}$ and $p38\alpha^{fl/fl}p38\beta^{fl/fl}GzmB^{cre/-}$ P14 naïve $CD8^+$ T cells were mixed at a 1:1 ratio, and then a total of 5×10^3 mixed cells was transferred to the recipient mice. The recipient mice were then infected with $LCMV_{Arm}$ the next day, and effector or memory $CD8^+$ T-cell responses were analyzed at the indicated time points. To assess the persistence of in vitro differentiated $CD8^+$ T cells, 3×10^6 cells of indicated genotypes were equally co-transferred into CD45.1 recipient mice, and donor cell persistence was evaluated the following day. To determine the secondary expansion, 5×10^4 P14 T cells were equally co-transferred into CD45.1 WT recipients. The recipient mice were then infected with $LCMV_{Arm}$ the following day and the mice were analyzed 7 days later.

Bone marrow reconstitution

To generate bone marrow chimeras, bone marrow cells from $p38\alpha^{fl/fl}p38\beta^{fl/fl}$ ($CD45.2^+CD90.2^+$) and $p38\alpha^{fl/fl}p38\beta^{fl/fl}GzmB^{cre/-}$ ($CD45.2^+CD90.1^+CD90.2^+$) mice (6 to 8 weeks old) were mixed at a 1:1 ratio, and a total of 1×10^7 cells was then transferred into lethally irradiated CD45.1 recipient mice (8Gys, RS2000, Rad Source). After 8 weeks for full bone marrow reconstitution, the chimeric mice were infected with $LCMV_{Arm}$, and the proportions of D^b-GP_{33-41}-$tetramer^+$ memory T cells were determined by flow cytometry at indicated time points.

In vitro differentiation system[28]

Purified splenic naïve P14 T cells of indicated genotypes were incubated with GP_{33-41} peptide (100 nM) and mIL-2 (100 ng/mL) in RPMI 1640 medium at a seeding density of 5×10^5 cells/mL for 2 days. The cultured cells were then washed twice and subsequently cultured in RPMI 1640 medium containing mIL-2 (100 ng/mL) for another 8 days, with medium being replaced every 2 days to maintain the mIL-2 concentration. The cultured cells were analyzed at days 2, 6, and 10 for viability detection, and at day 10 for subset differentiation and cytokine production.

RNA sequencing

For RNA sequencing (RNA-seq), naïve $CD8^+$ T cells were purified from spleens of untreated mice, or splenic D^b-GP_{33-41}-$tetramer^+$ $CD8^+$ T cells were sorted from $p38\alpha^{fl/fl}p38\beta^{fl/fl}$ and $p38\alpha^{fl/fl}p38\beta^{fl/fl}GzmB^{cre/-}$ mice at day 8 after $LCMV_{Arm}$ infection. RNA was extracted using RNAiso Plus (Takara Bio) and RNA-seq was performed by Majorbio or Novogene Corporation Inc. Genes with an average normalized read count >50 in each group were included in differential expression analysis. Differentially expressed genes (DEGs) were defined by using a $|\log_2$ fold change$| > 0.5$ and adjusted P value < 0.05 difference. The heatmaps consisting of DEGs displaying upregulation (red) or downregulation groups (blue) were ranked by a rise in P value. Volcano plots and heatmaps were generated using GraphPad Prism software, version 8.0. Gene Ontology (GO) enrichment analyses of differentially expressed genes

were carried out using NetworkAnalyst (https://www.networkanalyst.ca) with corrected P value <0.05.

Statistical analysis

Statistical analyses were performed on GraphPad Prism 8.0 software. P values were determined by using 2-tailed Student t-test. Statistical significance is considered as: not significant, $P \geq 0.05$; $^{*}P < 0.05$; $^{**}P < 0.01$; $^{***}P < 0.001$; and $^{****}P < 0.0001$.

Results

Selective *p38α/β* deletion in granzyme B–expressing cells modulates effector CD8+ T-cell fate

We employed the widely used $LCMV_{Arm}$ infection model to investigate the in vivo role of p38 signaling in CD8+ T cells. During the course of $LCMV_{Arm}$ infection, we observed a significant increase in both p38 and p-p38 protein levels in splenic CD8+ T cells from C57BL6/J WT mice (Fig. 1A). The

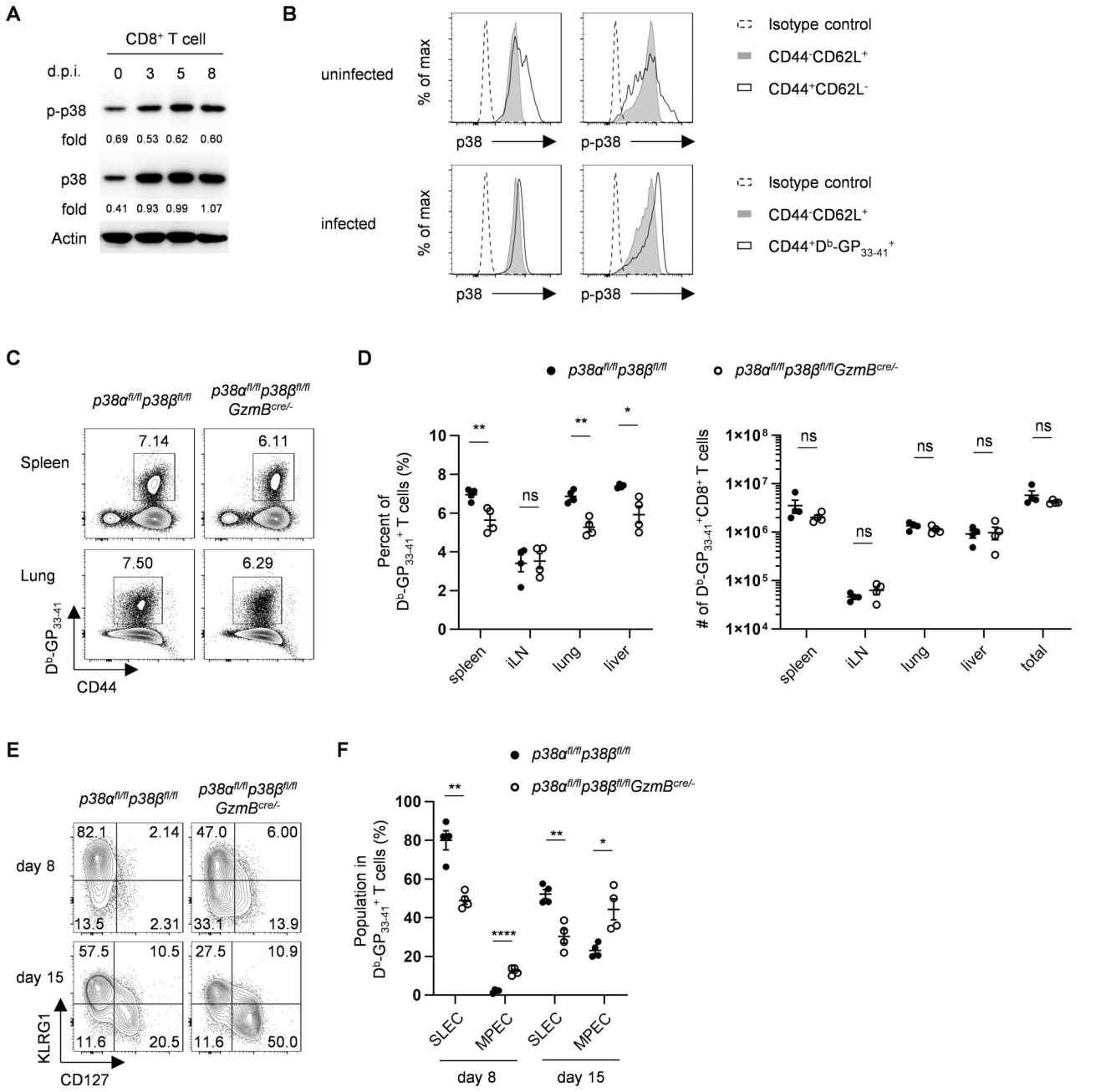

Figure 1. Modulating effector CD8+ T-cell fate through selective deletion of *p38α/β* in granzyme B–expressing cells. (A) Immunoblotting analysis depicts the expression levels of p38 and p-p38 in C57LB/6J WT mouse splenic CD8+ T cells at indicated days post–$LCMV_{Arm}$ infection (d.p.i.); relative expressions of p38 to actin and p-p38 to p38 are calculated as fold. (B) Intracellular staining of p38 and p-p38 in splenic naïve ($CD44^{-}CD62L^{+}$) and effector ($CD44^{+}CD62L^{-}$ for uninfected mice, $CD44^{+}D^{b}$-GP_{33-41}-tetramer+ for $LCMV_{Arm}$-infected mice at day 8) CD8+ T cells. Rabbit IgG was used as isotype control; representative plots are shown. (C and D) Representative plots of splenic and pulmonary antigen-specific CD8+ T cells ($CD44^{+}D^{b}$-GP_{33-41}-tetramer+) from $p38\alpha^{fl/fl}p38\beta^{fl/fl}$ and $p38\alpha^{fl/fl}p38\beta^{fl/fl}GzmB^{cre/-}$ mice 8 days post–$LCMV_{Arm}$ infection (C). D^{b}-GP_{33-41}-tetramer+ CD8+ T-cell frequencies and numbers in spleen, inguinal lymph node (iLN), lung, and liver ($n = 4$) (D). (E and F) Flow cytometry analysis of KLRG1 and CD127 expression on splenic D^{b}-GP_{33-41}-tetramer+ CD8+ T cells at days 8 and 15 post–$LCMV_{Arm}$ infection (E). Percentages of $KLRG1^{hi}CD127^{lo}$ (SLEC) and $KLRG1^{lo}CD127^{hi}$ (MPEC) populations in D^{b}-GP_{33-41}-tetramer+ CD8+ T cells ($n = 4$) (F). Values are represented as mean ± SEM. Data are representative of 2 or 3 independent experiments. Statistical analyses were performed with unpaired Student t-test. $^{*}P < 0.05$, $^{**}P < 0.01$, $^{****}P < 0.0001$; ns, not significant.

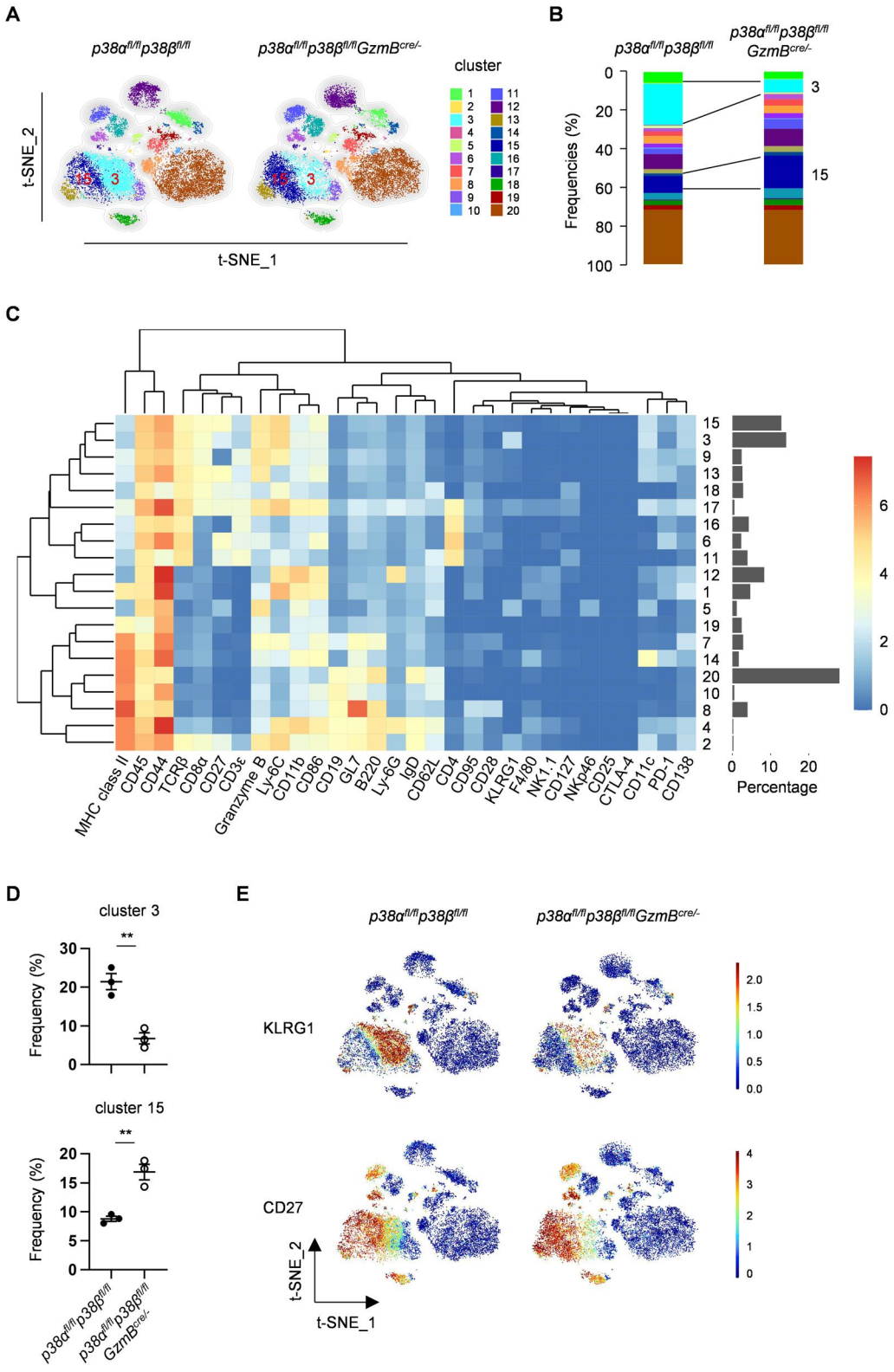

Figure 2. The alterations triggered by selective *p38α/β* deletion in granzyme B–expressing cells predominantly affect CD8$^+$ T cells. (A) Multidimensional CyTOF analysis of splenocytes from *p38α*$^{fl/fl}$*p38β*$^{fl/fl}$ and *p38α*$^{fl/fl}$*p38β*$^{fl/fl}$*GzmB*$^{cre/-}$ mice at day 8 post–LCMV$_{Arm}$ infection; clusters of leukocytes are displayed. (B) Mean frequencies of clusters correlating to (A) are shown. (C) Markers used for phenotyping of leukocytes in CyTOF analysis and correlating expression on various clusters. (D) Statistic comparison of cluster 3 and cluster 15 percentages in CyTOF analysis ($n = 3$). (E) Merged KLRG1 and CD27 expression on spleen leukocytes in CyTOF analysis. Values are represented as mean ± SEM. Statistical analyses were performed with unpaired Student *t*-test. $^{**}P < 0.01$.

rate of p38 phosphorylation appeared to be unchanged throughout the course since the increase in the level of p-p38 was contributed primarily by the elevation of p38 protein level (Fig. 1A). Flow cytometry analysis further confirmed that p38 and p-p38 levels were higher in antigen-specific effector CD8$^+$ T lymphocytes (D^b-GP$_{33-41}$-tetramer$^+$)

compared to their naïve counterparts (Fig. 1B), suggesting the participation of p38 signaling in the primary response of CD8$^+$ T cells. Additionally, analysis of naïve and effector CD8$^+$ T cells from noninfected WT mice showed modest upregulation of total p38, but not uniform activation of p-p38 (Fig. 1B), indicating that p38 expression can increase independently of LCMV infection, while phosphorylation is more likely linked to concurrent stimulation.

Given the widespread targeting of both p38α and p38β by most p38 inhibitors,[11] and the expression of both p38α and p38β in mature mouse CD8$^+$ T cells,[16] along with reported instances of their redundant function in many cases,[15] we first utilized mice with loxp-flanked alleles of *p38α* and *p38β*, crossed with mice expressing Cre-recombinase under the control of the human granzyme B (*GzmB*) promoter for further studies[23] (Fig. S1A). *GzmB-Cre* was used because granzyme B was reported to be selectively expressed in activated CD8$^+$ T cells.[23] However, efficient deletion of *p38α/β* in CD8$^+$ T cells was not only observed in LCMV$_{Arm}$-infected but also uninfected $p38\alpha^{fl/fl}p38\beta^{fl/fl}GzmB^{cre/-}$ mice (Fig. S1B), suggesting unexpected leaky Cre activity. The leakage was also evidenced by the observation of the early *p38α/β* deletion in thymic and peripheral T cells in $p38\alpha^{fl/fl}p38\beta^{fl/fl}GzmB^{cre/-}$ mice under homeostatic conditions (Fig. S1B, C). To assess whether *p38α/β* deletion affects T-cell development, we analyzed $p38\alpha^{fl/fl}p38\beta^{fl/fl}$ and $p38\alpha^{fl/fl}p38\beta^{fl/fl}GzmB^{cre/-}$ mice under homeostatic conditions. Thymocyte development—including double-negative, double-positive, and CD4 and CD8 single-positive T cells—was largely unperturbed, although a slight increase in double-positive T-cell frequency was observed (Fig. S1D, E). While a modest increase in peripheral CD4$^+$ T-cell frequency and a corresponding decrease in CD8$^+$ T-cell frequency were observed, total T-cell numbers remained comparable between genotypes (Fig. S1F, G). Notably, *p38α/β*-deficient mice exhibited an increased proportion of effector CD4$^+$ T cells and a reduction in the naïve subset, whereas CD8$^+$ T-cell subsets were unaffected in uninfected animals (Fig. S1H, I). To further define the impact of p38 in developmental maturation of CD8$^+$ T cells, we performed RNA-seq comparing $p38\alpha^{+/+}p38\beta^{+/+}$ and $p38\alpha^{-/-}p38\beta^{-/-}$ naïve CD8$^+$ T cells. Although a set of DEGs was detected, hallmark genes associated with naïve CD8$^+$ T-cell identity or essential regulators of CD8$^+$ T-cell development were not significantly altered. GO analysis revealed enrichment primarily in kinase-associated signaling pathways unrelated to CD8$^+$ T-cell activation and differentiation (Fig. S2A–C). Together, these data indicate that the early development and baseline transcriptional profile of CD8$^+$ T cells are largely preserved in *p38α/β*-deficient mice.

We then immunized both genotypes of mice with LCMV$_{Arm}$ and observed that the overall splenic CD8$^+$ T-cell response was not significantly affected by *p38α/β* deficiency, although the CD4$^+$ T-cell frequencies remained slightly elevated in the days following immunization (Fig. S3A, B). Analysis of LCMV$_{Arm}$-specific CD8$^+$ T cells using MHC-I D^b-GP$_{33-41}$ tetramer staining showed comparable numbers in lymphoid (spleen and inguinal lymph node) and nonlymphoid tissues (lung and liver) between $p38\alpha^{fl/fl}p38\beta^{fl/fl}GzmB^{cre/-}$ mice and control littermates, although the frequency of this clonotype was slightly reduced in the absence of *p38α/β* (Fig. 1C, D), indicating that p38 signaling is not essential for the overall generation of effector CD8$^+$ T cells. By day 15 postinfection, both the frequency and absolute number of D^b-GP$_{33-41}$-tetramer$^+$ CD8$^+$ T cells were comparable between *p38α/β*-deficient and control mice (Fig. S3C, D), further supporting that early differences do not impact the overall magnitude of the effector CD8$^+$ T-cell response. However, further characterization using KLRG1 and CD127 to define subsets of D^b-GP$_{33-41}$-tetramer$^+$ CD8$^+$ T cells revealed a reduction in SLECs and an increase in MPECs in *p38α/β*-deficient mice at days 8 and 15 postinfection (Fig. 1E, F). These findings highlight an important role of p38 signaling in determining the fate of effector CD8$^+$ T cells toward SLEC or MPEC phenotypes.

The changes in immune cell clusters caused by selective *p38α/β* deletion in granzyme B–expressing cells are primarily in CD8$^+$ T cells

The selective deletion of *p38α/β* in granzyme B–expressing cells resulted in altered differentiation of effector CD8$^+$ T cells following LCMV$_{Arm}$ infection. Given the actual expression of granzyme B in thymus T cells (Fig. S1C), but also its presence in natural killer cells and other cell types,[29] we sought to assess whether the knockout of *p38α/β* in granzyme B–expressing cells directly or indirectly influenced other immune cell subpopulations. To address this, we performed multidimensional time-of-flight mass cytometry (CyTOF) analysis on splenocytes isolated from $p38\alpha^{fl/fl}p38\beta^{fl/fl}GzmB^{cre/-}$ and control $p38\alpha^{fl/fl}p38\beta^{fl/fl}$ mice following LCMV$_{Arm}$ infection.

Utilizing t-SNE dimensionality reduction followed by group clustering, we observed no difference in the distribution of major immune cell types between $p38\alpha^{fl/fl}p38\beta^{fl/fl}GzmB^{cre/-}$ and $p38\alpha^{fl/fl}p38\beta^{fl/fl}$ mice (Fig. S4A). The frequencies of each immune cell subset in $p38\alpha^{fl/fl}p38\beta^{fl/fl}GzmB^{cre/-}$ mice resembled those in $p38\alpha^{fl/fl}p38\beta^{fl/fl}$ mice (Fig. S4B), as evidenced by the mapping of clusters correlating to different populations with marker intensity (Fig. 2C). Further analysis of the total landscape of spleen leukocytes revealed 2 subpopulations of CD8$^+$ T cells that exhibited marked differences between $p38\alpha^{fl/fl}p38\beta^{fl/fl}GzmB^{cre/-}$ and $p38\alpha^{fl/fl}p38\beta^{fl/fl}$ mice (Fig. 2A, B). Specifically, $p38\alpha^{fl/fl}p38\beta^{fl/fl}$ mice presented more cells in cluster 3 (defined by high expression of KLRG1) and fewer cells in cluster 15 (characterized by high expression of CD27) compared to $p38\alpha^{fl/fl}p38\beta^{fl/fl}GzmB^{cre/-}$ mice (Fig. 2D, E). The increased CD27 expression and decreased KLRG1 expression in these 2 clusters of *p38α/β*-deficient CD8$^+$ T cells support the earlier conclusion that p38α/β in effector CD8$^+$ T cells promotes short-lived effector cell generation.

p38 signaling is required for the optimal functional activation of effector CD8$^+$ T cells against selected epitopes

To investigate the impact of p38α and p38β on the functional activation of effector CD8$^+$ T cells, we analyzed the production of IFN-γ and TNF-α, key markers of CD8$^+$ T-cell activity in the LCMV$_{Arm}$ infection model. On day 8 postinfection, splenocytes from both $p38\alpha^{fl/fl}p38\beta^{fl/fl}GzmB^{cre/-}$ and $p38\alpha^{fl/fl}p38\beta^{fl/fl}$ mice were stimulated with LCMV-derived peptides GP$_{33-41}$ and NP$_{396-404}$. The proportions of IFN-γ– and TNF-α–producing CD8$^+$ T cells were slightly lower in response to the GP$_{33-41}$ peptide in *p38α/β*-deficient mice compared to WT controls, while no significant difference was observed in response to the NP$_{396-404}$ peptide (Fig. 3A, B). Moreover, the absolute numbers of cytokine-producing CD8$^+$ T cells were

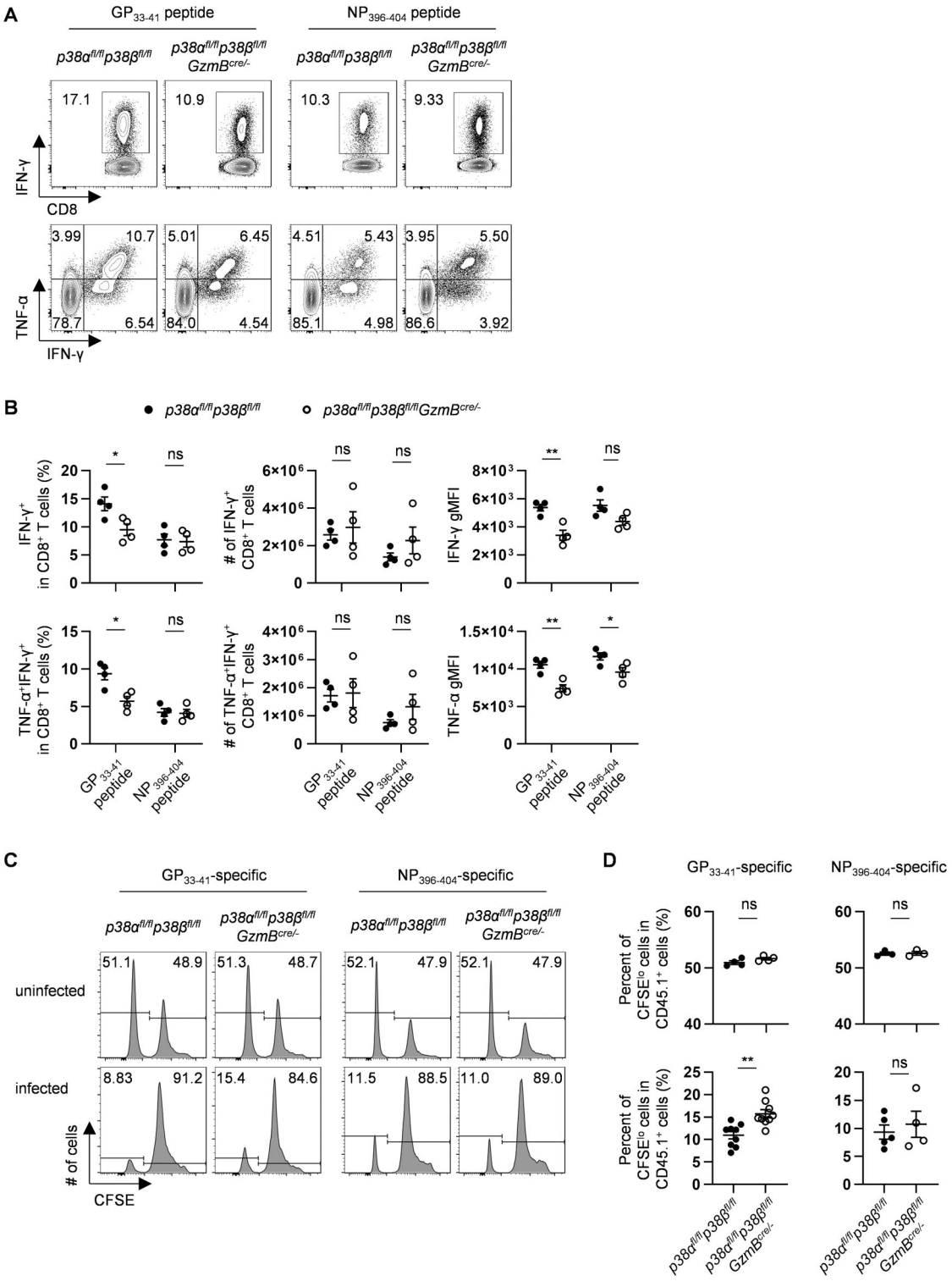

Figure 3. p38 signaling is required for the optimal functional activation of certain epitope-specific effector CD8$^+$ T cells. (A and B) Splenocytes from *p38α*$^{fl/fl}$*p38β*$^{fl/fl}$ and *p38α*$^{fl/fl}$*p38β*$^{fl/fl}$*GzmB*$^{cre/-}$ mice at day 8 post–LCMV$_{Arm}$ infection were intracellularly stained for IFN-γ and TNF-α production after in vitro peptide stimulation, plots were gated on CD8$^+$ T cells (A). Frequencies and numbers of splenic IFN-γ$^+$ CD8$^+$ T cells, gMFI of IFN-γ, percentages and numbers of TNF-α and IFN-γ–coproducing CD8$^+$ T cells, and TNF-α gMFI were calculated ($n = 4$) (B). (C and D) Representative plots of in vivo killing results conducted on uninfected and LCMV$_{Arm}$-infected mice at day 8, with the percentages of splenic CFSE^{lo} GP$_{33-41}$ or NP$_{396-404}$ peptide–pulsed target cells in transferred cells used to calculate antigen-specific killing activity (C). Statistics of antigen-specific killing activity ($n = 3$ to 9) (D). Values are represented as mean ± SEM. Data are representative of 2 or 3 independent experiments. Statistical analyses were performed with unpaired Student *t*-test. $^*P < 0.05$, $^{**}P < 0.01$; ns, not significant.

comparable between the 2 groups (Fig. 3B). Furthermore, expression levels of IFN-γ and TNF-α (measured by geometric mean fluorescence intensity [gMFI]) in *p38α*$^{-/-}$*p38β*$^{-/-}$ effector CD8$^+$ T cells were generally lower than those in *p38α*$^{+/+}$*p38β*$^{+/+}$ cells, particularly in response to the GP$_{33-41}$ peptide (not obvious for NP$_{396-404}$ peptide–specific IFN-γ

production), indicating that p38 signaling may enhance CTL activity in an epitope-dependent manner (Fig. 3B). We further analyzed IFN-γ and TNF-α production in D^b-GP$_{33-41}$-tetramer$^+$ CD8$^+$ T cells. At day 8 postinfection, the proportions of IFN-γ$^+$ and TNF-α$^+$ cells were comparable between *p38α/β*-deficient and control mice (Fig. S5A, B). By day 15, the knockout group showed a modest reduction in both the frequency and gMFI of IFN-γ$^+$ and TNF-α$^+$ cells, with no alterations on numbers (Fig. S5C, D). These data suggest a slight increase in the number of splenocytes in conditional knockout mice. The reduced frequency likely reflects a subtle shift in cellular composition rather than a substantial loss of effector cells. Additionally, within the D^b-GP$_{33-41}$-tetramer$^+$ CD8$^+$ T-cell population, IFN-γ and TNF-α production also showed a modest decrease in *p38α/β*-deficient cells at day 15 (Fig. S5E, F). Overall, the impact of *p38α/β* deficiency on cytokine production was modest, and further studies are needed to determine whether these differences significantly impair CTL functionality.

To further assess the functional role of p38α/β in effector CD8$^+$ T-cell cytotoxicity, we then evaluated the in vivo killing ability of CTLs. CD45.1 splenocytes, either pulsed with peptide or unpulsed, were labeled with varying intensities of CFSE, mixed equally and co-transferred into uninfected or LCMV$_{Arm}$-infected mice at day 8 postinfection. The antigen-specific cytolytic activity of CD8$^+$ T cells was measured by analyzing the proportion of donor cells with low CFSE intensity. No basal killing activity against antigen-loaded cells in uninfected mice was observed (Fig. 3C, D). Upon infection, *p38α$^{fl/fl}$p38β$^{fl/fl}$GzmB$^{cre/-}$* mice retained a higher proportion of GP$_{33-41}$ peptide–loaded target cells in their spleens compared to *p38α$^{fl/fl}$p38β$^{fl/fl}$* mice, indicating reduced cytolytic activity of GP$_{33-41}$-specific CD8$^+$ T cells in the absence of *p38α/β*. In contrast, killing of NP$_{396-404}$ peptide–loaded targets was unaffected (Fig. 3C, D). Therefore, *p38α/β* deletion compromises the cytotoxic capability of effector CD8$^+$ T cells against selected epitopes.

Transcriptional regulation of effector CD8$^+$ T-cell differentiation by p38 signaling

To investigate the mechanistic role of the p38 signaling pathway in the differentiation of effector CD8$^+$ T cells, D^b-GP$_{33-41}$-specific CD8$^+$ T cells were isolated from both WT and *p38α/β*-deficient mice (*p38α$^{fl/fl}$p38β$^{fl/fl}$* and *p38α$^{fl/fl}$p38β$^{fl/fl}$GzmB$^{cre/-}$*, respectively) at day 8 postinfection with LCMV$_{Arm}$, and applied to RNA-seq analysis. With a cutoff of >0.5 log$_2$ fold change, 62 upregulated and 51 downregulated genes were found in *p38α/β*-deficient effector CD8$^+$ T cells when compared with their WT counterparts (Fig. 4A and Fig. S6A). GO analysis revealed that DEGs were enriched in biological processes of protein phosphorylation regulation controlling multiple signaling pathways (eg *Map3k5*, *Map2k6*, *Dusp16*, *Srcin1*). Enriched GO terms also included those related to T-cell activation and migration (eg *Cd24a*, *Cd27*, *Lag3*, *Ctla4*, *Jaml*, *Sell*, *Tnfrsf18*, *Cxcr3*) (Fig. 4B). In addition, these DEGs were mainly enriched in plasma membrane components acting as cell surface receptors for immunomodulators (eg *Il7r*, *Cd244a*, *Nrp1*, *Notch3*, *Slamf6*) (Fig. 4B), suggesting that p38α/β might be involved in modulating CD8$^+$ T-cell responsiveness to extracellular signals.

Further in-depth analysis of these genes highlighted the transcriptional shifts associated with *p38α/β* deficiency. Aligning with prior phenotyping results, mRNA levels of

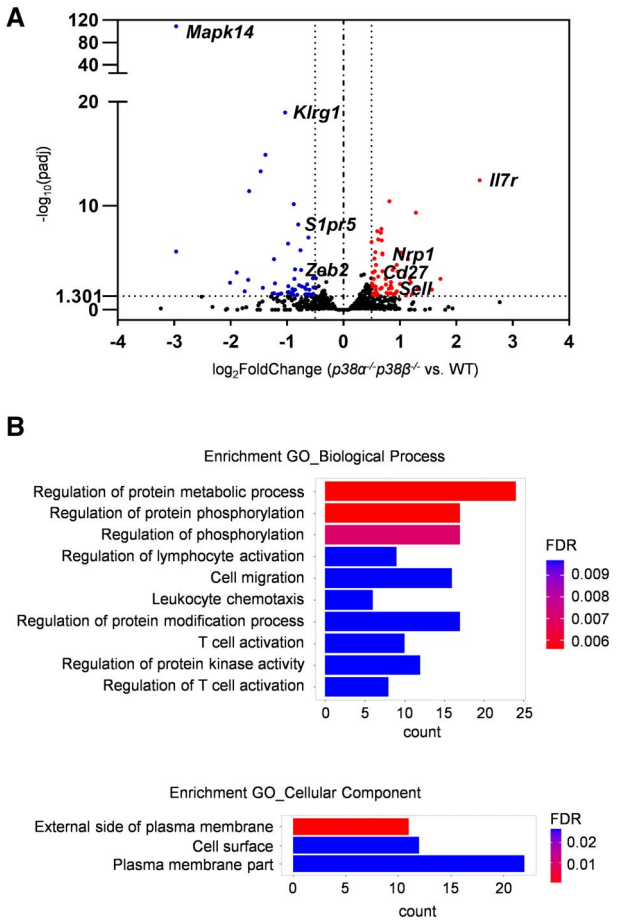

Figure 4. Transcriptional regulation of effector CD8$^+$ T-cell differentiation by p38 signaling. (A) Splenic D^b-GP$_{33-41}$-tetramer$^+$ CD8$^+$ T cells sorted from LCMV$_{Arm}$-infected *p38α$^{fl/fl}$p38β$^{fl/fl}$* and *p38α$^{fl/fl}$p38β$^{fl/fl}$GzmB$^{cre/-}$* mice at day 8 were subjected to RNA-seq. A volcano plot comparing DEGs between *p38α$^{+/+}$p38β$^{+/+}$* and *p38α$^{-/-}$p38β$^{-/-}$* cells was generated, with selected p38 target genes indicated ($n = 4$). (B) GO enrichment analysis of DEGs in RNA-seq data reveals the top 10 biological processes and the cellular components correlated with the differential gene expression profiles. FDR, false discovery rate.

genes typically associated with effector function, such as *Klrg1*, *Cd24a*, and *Zeb2*,[30–32] were decreased, whereas those linked to a memory phenotype, including *Il7r*, *Cd27*, *Sell*, and *Cxcr3*,[33–36] were increased in *p38α/β*-deficient antigen-specific CD8$^+$ T cells, confirming findings from flow cytometry analysis (Fig. S6B, C). Additionally, genes reported to foster memory cell formation, such as *Nrp1* and *Spi2A*,[37,38] were upregulated in *p38α/β*-deficient CD8$^+$ T cells, while *S1pr5*, a gene known to facilitate peripheral T-cell tissue emigration,[39] was downregulated. Expression of various immune regulatory receptors was also affected by *p38α/β* deficiency, including upregulation of co-stimulatory molecules such as *Cd27*, *Jaml*, and *Gitr*,[40,41] as well as differential modulation of co-inhibitory receptors—marked by increased expression of *Slamf6*, *Lag3*, and *Ctla4* and reduced level of *2B4*[42–45] (Fig. S6C)—reflecting a potential regulatory role of the p38 pathway in modulating stimulatory and inhibitory signals within CD8$^+$ T cells. However, the surface protein levels of SLAMF6 and LAG3 appeared low and showed only minor differences between genotypes (Fig. S6B), indicating that the functional relevance of these transcriptional changes may be limited or context-dependent. Interestingly, *p38α/β* deletion

led to elevated expression of *Map3k5* and *Map2k6*, genes encoding upstream kinases that activate p38,[11] suggesting a possible compensatory feedback mechanism.

Collectively, while these data demonstrate that p38α/β is required for optimal induction of effector programs, they do not exclude the possibility that enhanced memory precursor formation may result indirectly from impaired effector differentiation rather than from a direct suppressive role of p38α/β on memory programming. The observed transcriptional shifts may reflect weakened TCR or co-stimulatory signals in the absence of *p38α/β*, which favor incomplete terminal differentiation and a bias toward memory precursor fates. Thus, p38α/β appears to contribute to effector/memory fate decisions primarily by promoting effector differentiation, and its absence allows for accumulation of cells with memory-like features.

p38α/β deletion favors central memory T-cell generation

It is well-documented that a subset of antigen-experienced $CD8^+$ T cells survive the contraction phase and differentiate into memory cells in the $LCMV_{Arm}$ infection model.[24] Given our earlier observation that *p38α/β* deficiency promotes the generation of MPECs (Fig. 1E, F) and that inhibition of p38 signaling favors the differentiation of cultured $CD8^+$ T cells toward a Tcm-like phenotype in vitro,[21] we next explored long-term memory $CD8^+$ T-cell formation in $p38\alpha^{fl/fl}p38\beta^{fl/fl}GzmB^{cre/-}$ mice. 60 days post–$LCMV_{Arm}$ infection, the percentages and numbers of LCMV-specific memory $CD8^+$ T cells were similar between $p38\alpha^{fl/fl}p38\beta^{fl/fl}GzmB^{cre/-}$ and $p38\alpha^{fl/fl}p38\beta^{fl/fl}$ mice (Fig. 5A, B). Additionally, the proportions and counts of IFN-γ– and TNF-α–producing memory $CD8^+$ T cells in spleens of $p38\alpha^{fl/fl}p38\beta^{fl/fl}GzmB^{cre/-}$ mice were comparable to those of their WT counterparts, mirroring earlier findings where *p38α/β*-deficient CTLs expressed lower levels of IFN-γ and TNF-α than WT cells under specific peptide stimulation (Fig. S7A, B). Consequently, we further examined the differentiation state of memory $CD8^+$ T cells to gain deeper insights.

Central memory T cells, characterized by high expression level of CD62L and proliferating robustly upon cognate antigen reencounter,[46] are a major subset of memory T cells that predominantly localize within secondary lymphoid organs. As shown in Fig. 5C and D, the $p38\alpha^{fl/fl}p38\beta^{fl/fl}GzmB^{cre/-}$ mice exhibited a significant increase of $CD62L^{hi}$ Tcm cells in their spleens compared to $p38\alpha^{fl/fl}p38\beta^{fl/fl}$ mice over time after infection, indicating an enhancement in Tcm cell formation. Apart from promoting the differentiation of $CD8^+$ Tcm cells, *p38α/β* deficiency also enhanced IL-2 production, a key factor for robust secondary expansion of memory T cells upon antigen reencounter.[10] The frequencies of antigen-specific IL-2–producing $CD8^+$ T cells were significantly increased in $p38\alpha^{fl/fl}p38\beta^{fl/fl}GzmB^{cre/-}$ mice, compared to their $p38\alpha^{fl/fl}p38\beta^{fl/fl}$ counterparts at both early and late time points postinfection, although the per-cell IL-2 expression level remained comparable between genotypes (Fig. 5E, F). These findings indicate that p38 signaling restricts both the development of $CD8^+$ Tcm cells and their associated functional potential, underscoring its role in shaping the memory differentiation landscape.

Enhanced secondary response by *p38α/β*-deficient memory $CD8^+$ T cells

Given that more Tcm cells were generated in $p38\alpha^{fl/fl}p38\beta^{fl/fl}GzmB^{cre/-}$ mice in the primary response, we sought to investigate whether $p38\alpha^{fl/fl}p38\beta^{fl/fl}GzmB^{cre/-}$ mice gave rise to a better outcome upon recall response. To exclude the possible irrelevant preexisting immunity, mice previously infected with $LCMV_{Arm}$ were rechallenged with *L. monocytogenes* engineered to express the LCMV epitope GP_{33-41} peptide (Lm-gp33), and pathogen-specific tetramer positive $CD8^+$ T cells in spleen were measured. By day 7 after rechallenge, $p38\alpha^{fl/fl}p38\beta^{fl/fl}GzmB^{cre/-}$ mice possessed a higher proportion and larger number of D^b-GP_{33-41}-specific $CD8^+$ T cells in their spleens compared to controls (Fig. 6A, B), suggesting a suppressive function of p38α/β in memory $CD8^+$ T-cell secondary response. Moreover, the proportions of secondary effector $CD8^+$ T cells differentiating into SLEC ($KLRG1^{hi}CD127^{lo}$) and MPEC ($KLRG1^{lo}CD127^{hi}$) subsets were comparable between WT and *p38α/β*-deficient mice, suggesting that p38 signaling does not significantly influence the fate decision of effector $CD8^+$ T cells during the recall response (Fig. S8A, B).

We next investigated the clearance ability of expanded $CD8^+$ T cells in the secondary response in these mice, and the in vivo killing assay was performed one week after antigenic rechallenge. As expected, *p38α/β* deficiency in $CD8^+$ T cells facilitated a more efficient elimination of target cells, evidenced by a reduced presence of antigen peptide–loaded foreign splenocytes in rechallenged $p38\alpha^{fl/fl}p38\beta^{fl/fl}GzmB^{cre/-}$ mice (Fig. 6C, D). However, when cytolytic function was assessed in vitro using equal numbers of recalled $CD8^+$ T cells and GP_{33-41} peptide–loaded EL4 cells, *p38α/β*-deficient secondary effector $CD8^+$ T cells displayed reduced killing activity on a per-cell basis (Fig. S8C). These results suggest that the enhanced expansion of memory $CD8^+$ T cells in *p38α/β*-deficient mice may compensate for their diminished individual cytolytic capacity, resulting in overall improved target clearance in vivo. Nevertheless, it remains possible that under conditions of limited memory T-cell availability, such as after suboptimal priming or low precursor frequency, the observed reduction in cytokine production could become biologically more consequential. This highlights a regulatory role of p38 signaling in balancing memory $CD8^+$ T-cell quantity and per-cell functional quality during recall responses.

The role of p38α/β in Tcm and MPEC generation is cell-intrinsic

Considering the possible interplays between $CD8^+$ T cells and their external environment, we made a setting in which WT and *p38α/β*-deficient $CD8^+$ T cells coexisted. Chimeric mice with mixed bone marrow were generated by transferring equal numbers of bone marrow cells from $p38\alpha^{fl/fl}p38\beta^{fl/fl}$ and $p38\alpha^{fl/fl}p38\beta^{fl/fl}GzmB^{cre/-}$ mice into lethally irradiated recipients. Following full reconstitution, these bone marrow chimeric mice were infected with $LCMV_{Arm}$, and memory $CD8^+$ T-cell formation was assessed. The reconstitution efficiency was robust, reaching at least 90% (Fig. S9A, B), and total $CD8^+$ T-cell populations developed similarly regardless of genotype (Fig. S9C, D). Comparable frequencies of D^b-GP_{33-41}-specific $CD8^+$ T cells arising from either WT or *p38α/β*-deficient bone marrow were observed in the same host (Fig. 7A, B). Still, *p38α/β*-deficient antigen-specific $CD8^+$ T cells exhibited a higher proportion of $CD62L^{hi}$ cells compared to WT

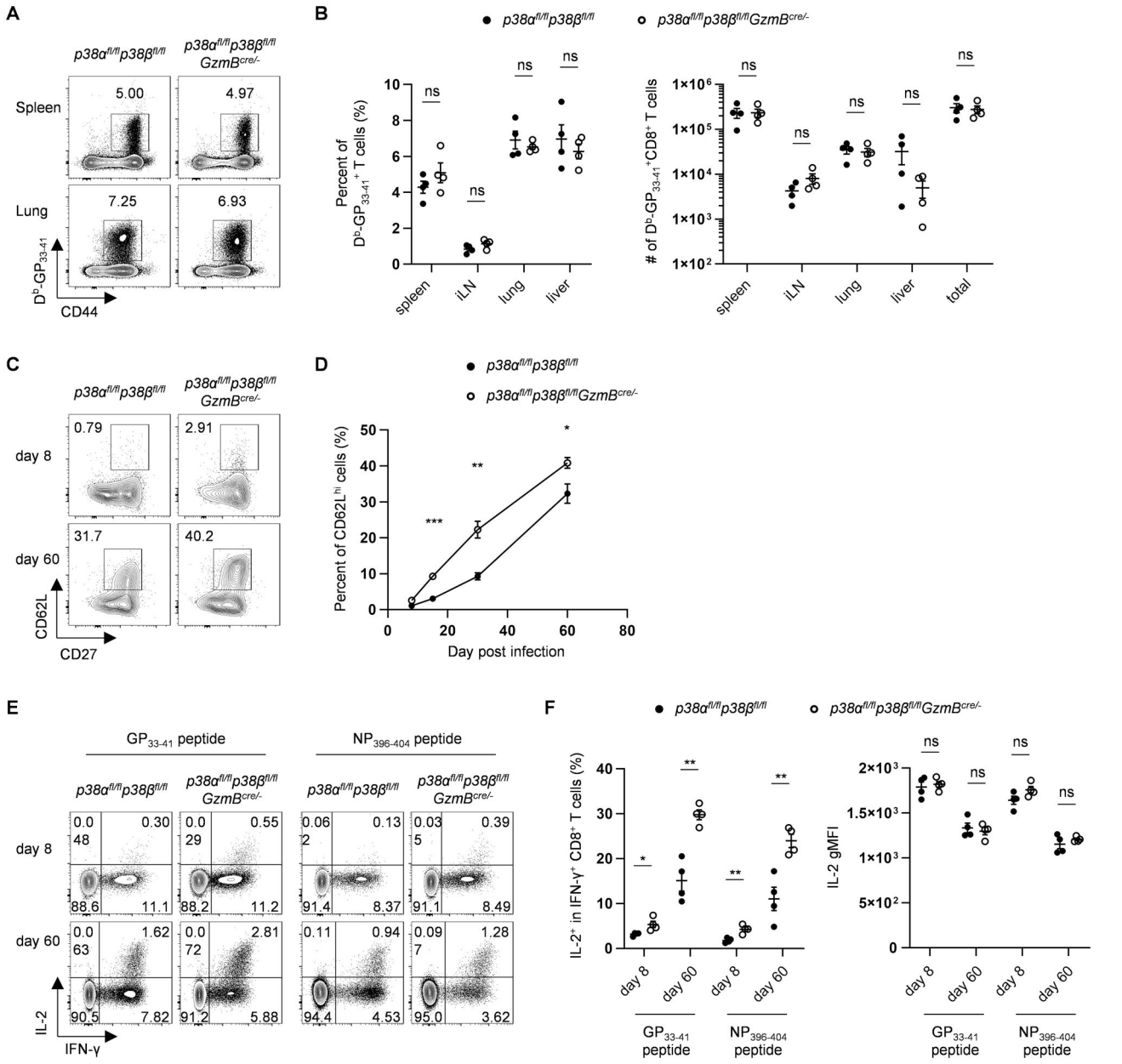

Figure 5. *p38α/β* deletion favors central memory T-cell generation and IL-2 production. (A and B) Representative plots depict splenic and pulmonary CD44$^+$D^b-GP$_{33-41}$-tetramer$^+$ cells in CD8$^+$ T cells from *p38α$^{fl/fl}$p38β$^{fl/fl}$* and *p38α$^{fl/fl}$p38β$^{fl/fl}$GzmB$^{cre/-}$* mice 60 days post–LCMV$_{Arm}$ infection (A). D^b-GP$_{33-41}$-tetramer$^+$ CD8$^+$ T-cell percentages and numbers in spleen, inguinal lymph node (iLN), lung, and liver were quantified ($n = 4$) (B). (C) Expression of CD27 and CD62L on splenic D^b-GP$_{33-41}$-tetramer$^+$ CD8$^+$ T cells at days 8 and 60 post–LCMV$_{Arm}$ infection. (D) Percentages of CD62L^{hi} cells (Tcm) in splenic D^b-GP$_{33-41}$-tetramer$^+$ CD8$^+$ T cells at the indicated days postinfection ($n = 4$ to 7). (E and F) Splenocytes from *p38α$^{fl/fl}$p38β$^{fl/fl}$* and *p38α$^{fl/fl}$p38β$^{fl/fl}$GzmB$^{cre/-}$* mice at days 8 and 60 post–LCMV$_{Arm}$ infection were intracellularly stained for IFN-γ and IL-2 production after in vitro peptide stimulation; plots were gated on CD8$^+$ T cells (E). Percentage of IL-2–producing cells in IFN-γ$^+$ CD8$^+$ T cells and IL-2 gMFI were calculated ($n = 4$) (F). Values are represented as mean ± SEM. Data are representative of 2 or 3 independent experiments. Statistical analyses were performed with unpaired Student *t*-test. $^*P < 0.05$, $^{**}P < 0.01$, $^{***}P < 0.001$; ns, not significant.

counterparts, confirming that p38α/β restricted Tcm cell formation (Fig. 7C, D).

Furthermore, we isolated congenic marked naive *p38α$^{fl/fl}$p38β$^{fl/fl}$P14* and *p38α$^{fl/fl}$p38β$^{fl/fl}$GzmB$^{cre/-}$P14* CD8$^+$ T cells, mixed them equally, and adoptively transferred to recipient mice followed by LCMV$_{Arm}$ infection. CD8$^+$ T-cell responses of donor cells were then analyzed at the indicated time points postinfection. Both WT and *p38α/β*-deficient donor cells exhibited comparable expansion kinetics and long-term persistence (Fig. S9E, F and Fig. 7E, F). To further confirm the cell-intrinsic role of p38α/β in effector CD8$^+$ T-cell differentiation, we also analyzed the expression of KLRG1 and CD127. Notably, a significant augmentation of the MPEC population and a concomitant decrease in the SLEC population were evident in *p38α/β*-deficient P14 donor cells at day 8 postinfection (Fig. S9G, S9H), consistent with our previous findings. Furthermore, a higher proportion of *p38α/β*-deficient memory P14 donor cells exhibited the capability to produce IL-2 (Fig. 7G, H), and a modest increase in IFN-γ–producing cells was also observed, albeit without significant changes in per-cell cytokine expression levels (Fig. S9I, J). Collectively, these observations revealed a cell-intrinsic

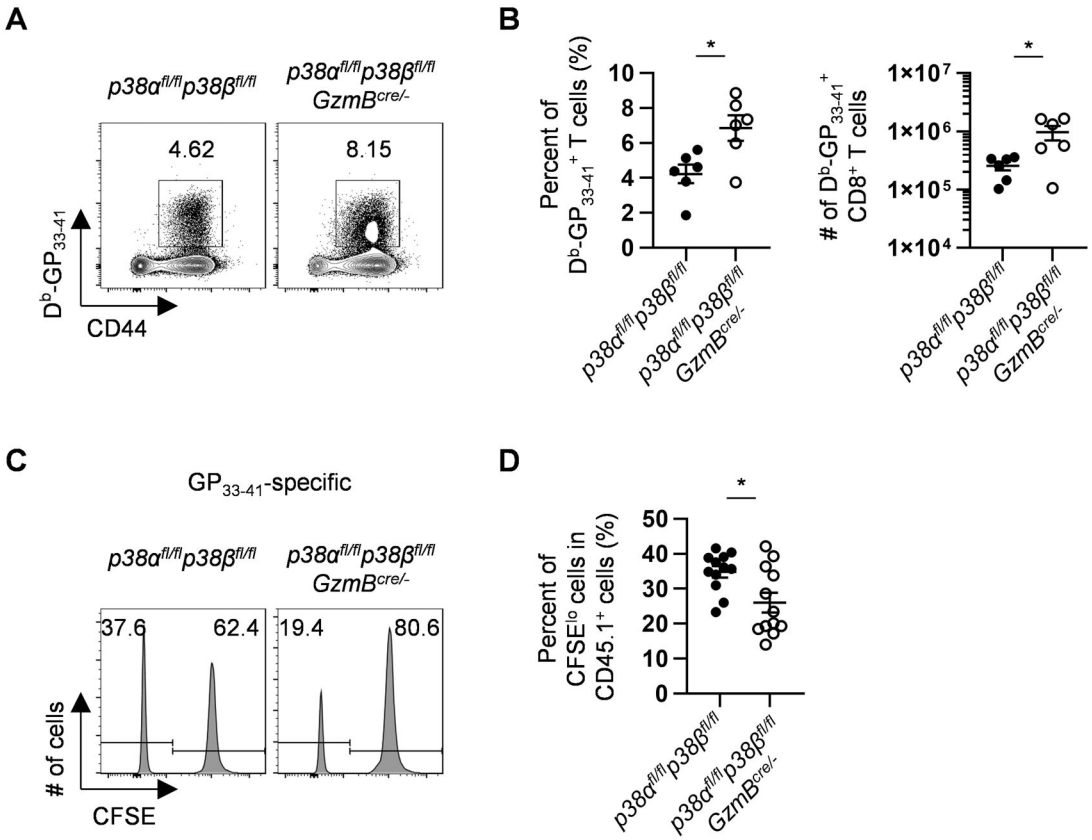

Figure 6. Enhanced secondary response by *p38α/β*-deficient memory CD8$^+$ T cells. (A and B) Representative plots of splenic CD44$^+$D^b-GP$_{33-41}$-tetramer$^+$ cells gated on CD8$^+$ T cells at day 7 after Lm-gp33 rechallenge in mice previously infected with LCMV$_{Arm}$ 60 days before (A). Frequencies and numbers of D^b-GP$_{33-41}$-tetramer$^+$ CD8$^+$ T cells in spleen ($n = 6$) (B). (C and D) Representative plots of in vivo killing results conducted on Lm-gp33 rechallenged mice at day 7, with the percentages of splenic CFSE^{lo} GP$_{33-41}$ peptide–pulsed target cells in transferred cells used to calculate antigen-specific killing activity (C). Statistics of antigen-specific killing activity ($n = 12$) (D). Values are represented as mean ± SEM. Data are representative of 2 independent experiments. Statistical analyses were performed with unpaired Student *t*-test. $^*P < 0.05$.

role for p38 signaling in limiting MPEC and central memory CD8$^+$ T-cell differentiation.

p38α/β deletion improves persistence and function of in vitro expanded CD8$^+$ T cells

Central memory T cells possess superior persistence and enhanced antitumor immunity compared to effector T cells in adoptive cell transfer (ACT) therapy,[47] and recent studies have shown that p38 inhibitor treatment enhances the efficacy of ACT therapy.[21,22] Building upon these findings and our endogenous genetic data, we investigated whether *p38α/β* deficiency could induce similar effects on in vitro expanded CD8$^+$ T cells.

We applied an in vitro expansion scheme for P14 CD8$^+$ T cells of the indicated genotypes, modeled on clinically relevant procedures.[28] After antigen-specific activation and IL-2–driven expansion, cell viability was well-maintained, with no significant differences observed between the 2 genotypes (Fig. S10A, B); analogously, *p38α/β* deletion reduced CD8$^+$ T-cell effector differentiation while promoting a central memory–like phenotype in the in vitro differentiation system (Fig. 8A, B). Interestingly, the proportions of IFN-γ and TNF-α–co-producing cells remained unaffected by *p38α/β* deficiency but, different from the endogenous settings, *p38α/β* deletion elevated the IFN-γ expression level while reducing the TNF-α expression level in CD8$^+$ T cells in the in vitro culture (Fig. S10C, D).

Subsequently, the in vitro expanded P14 T cells with indicated genotypes were adoptively co-transferred into receipt mice, and their homeostatic persistence and responsiveness to infection were assessed. Unexpectedly, in vitro expanded *p38α/β* knockout CD8$^+$ T cells demonstrated superior engraftment and persistence relative to their WT counterparts in the host (Fig. 8C, D). Nevertheless, both cells maintained an according central memory phenotype in vivo (Fig. S10E, F), and the numerical advantage of the knockout cells after LCMV$_{Arm}$ infection reflected their initial engraftment ratios (Fig. 8E, F). Furthermore, the killing ability of the in vitro differentiated P14 T cells was also verified. Recipient mice transferred with cultured *p38α/β*-deficient P14 T cells exhibited a reduced LCMV$_{Cl13}$ burden in the blood compared with those transferred with WT P14 T cells in the chronic LCMV$_{Cl13}$ infection model (Fig. 8G). Thus, *p38α/β* deficiency conferred significant benefits on in vitro differentiated CD8$^+$ T cells in the engraftment outcome in vivo, and Tcm generation likely plays an important role in the beneficial effects of p38 inhibition in adoptive T-cell transfer therapy.

Depletion of *p38α* is primarily responsible for promoting MPEC formation in *p38α/β* double-deficient CD8$^+$ T cells

p38α and p38β are the closest homologues within the p38 MAPK family, and several studies have demonstrated specific functions of p38α or p38β in several processes,[48] and the

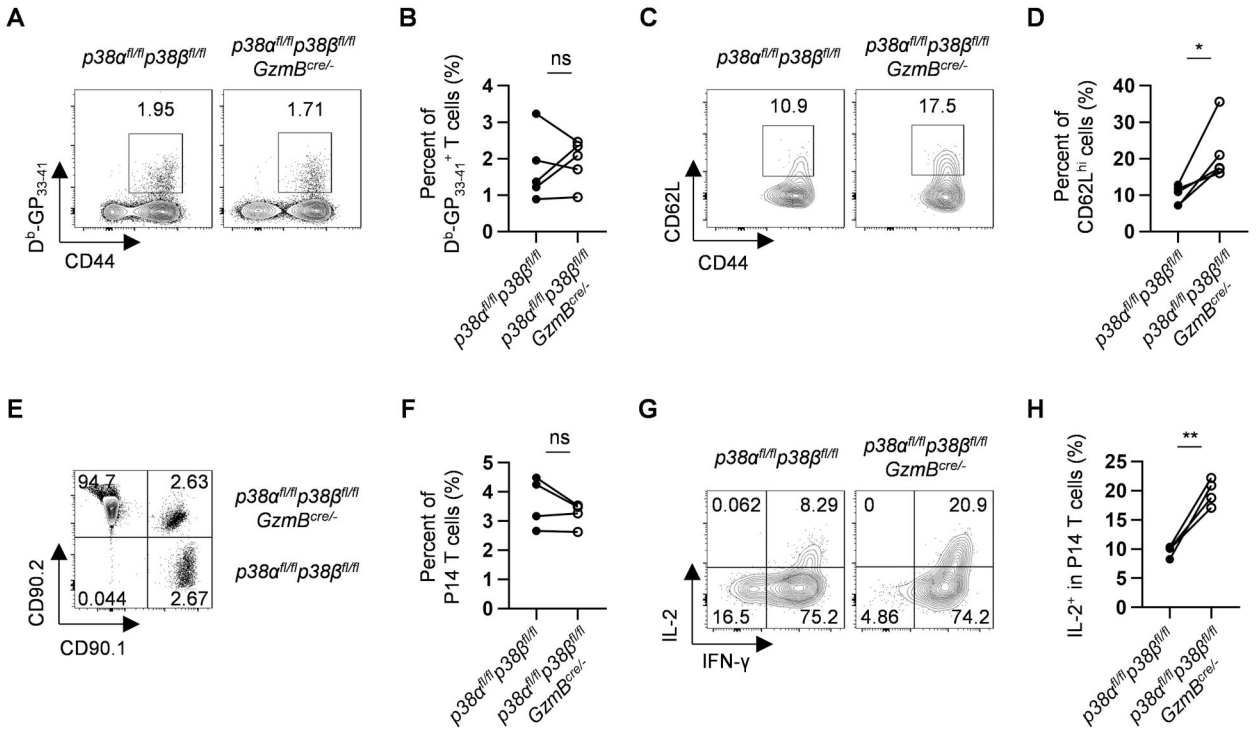

Figure 7. The role of p38α/β in Tcm differentiation and IL-2 production is cell-intrinsic. (A–D) Bone marrow chimeric mice were immunized with $LCMV_{Arm}$, and 35 days later, the plots of splenic D^b-GP_{33-41}-tetramer$^+$ CD8$^+$ T cells originally derived from cognate mice are shown (A). Percentages of CD44$^+$$D^b$-$GP_{33-41}$-tetramer$^+$ cells in cognate CD8$^+$ T cells were calculated ($n = 5$) (B). Plots show CD62L expression in cognate D^b-GP_{33-41}-tetramer$^+$ CD8$^+$ T cells (C). Percentages of CD62L^{hi} populations in cognate D^b-GP_{33-41}-tetramer$^+$ CD8$^+$ T cells were calculated ($n = 5$) (D). (E–H) *p38α$^{fl/fl}$p38β$^{fl/fl}$* (*CD90.1/CD90.1*) and *p38α$^{fl/fl}$p38β$^{fl/fl}$GzmB$^{cre/-}$* (*CD90.1/CD90.2*) naïve P14 T cells were co-transferred at 1:1 ratio into recipient mice (*CD90.2/CD90.2*), subsequently infected with $LCMV_{Arm}$, and analyzed 30 days later. Plots show P14 T-cell frequencies in splenic CD8$^+$ T cells (E). Percentages of P14 T cells were calculated (F). Intracellular staining for IFN-γ and IL-2 production in P14 donor cells (G). Percentages of IL-2–producing cells in P14 donor cells ($n = 4$) (H). Data are representative of 2 independent experiments. Statistical analyses were performed with paired Student *t*-test. $^*P < 0.05$, $^{**}P < 0.01$; ns, not significant.

detailed roles of p38α and p38β in CD8$^+$ T-cell response require further elucidation. To address this, we generated *p38α*-specific knockout (*p38α$^{fl/fl}$GzmB$^{cre/-}$*) or *p38β*-specific knockout (*p38β$^{fl/fl}$GzmB$^{cre/-}$*) mice and subjected them to $LCMV_{Arm}$ infection.

Consistent with observations in *p38α$^{fl/fl}$p38β$^{fl/fl}$GzmB$^{cre/-}$* mice, *p38α* deletion modestly reduced the frequency but did not affect the absolute number of virus-specific effector CD8$^+$ T cells, as evidenced by comparable numbers of splenic D^b-GP_{33-41}-tetramer$^+$ CD8$^+$ T cells in *p38α$^{fl/fl}$* and *p38α$^{fl/fl}$GzmB$^{cre/-}$* mice (Fig. 9A, B). Notably, *p38α$^{fl/fl}$GzmB$^{cre/-}$* mice exhibited reduced SLEC but increased MPEC frequencies in comparison with their WT counterparts (Fig. 9C, D). While cytokine-producing CD8$^+$ T-cell frequencies were only slightly diminished following GP_{33-41} peptide stimulation, not $NP_{396-404}$ peptide, the overall numbers of virus-specific IFN-γ– and TNF-α–producing CD8$^+$ T cells were comparable between *p38α$^{fl/fl}$* and *p38α$^{fl/fl}$GzmB$^{cre/-}$* mice (Fig. 9E, F). However, per-cell cytokine production was reduced in *p38α*-deficient CD8$^+$ T cells, with lower IFN-γ and TNF-α expression levels in response to GP_{33-41} and, to a lesser extent, $NP_{396-404}$ peptide (Fig. 9F). The decreased tendency in the expression levels of IFN-γ and TNF-α in *p38α$^{-/-}$* cells is lower compared to that observed in *p38α$^{-/-}$p38β$^{-/-}$* cells. Conversely, when comparing *p38β$^{fl/fl}$* and *p38β$^{fl/fl}$GzmB$^{cre/-}$* mice in terms of their LCMV-specific CD8$^+$ T-cell clonal expansion, differentiation, and cytokine production, we did not find statistically relevant effects of *p38β* deletion (Fig. S11A–F). Taken together, these data underscore that p38α plays a predominant role in restraining MPEC generation, while p38β only exhibits minor redundant function of p38α in effector cytokine production.

Discussion

In this study, we have provided new insights into the critical role of intracellular p38 signaling in regulating effector and memory CD8$^+$ T-cell differentiation during antiviral immune responses. To overcome the embryonic lethality associated with global *p38α* deletion, we employed the Cre-loxP system to specifically ablate *p38α* and *p38β* in CD8$^+$ T cells. Although GzmB-Cre is primarily reported to be active in activated CD8$^+$ T cells,[23] we observed leaky Cre activity leading to unintended deletion of p38 in thymic T cells (Fig. S1B), consistent with previously reported findings that GzmB-Cre can mediate recombination in a broad range of hematopoietic cells depending on the specific floxed allele and experimental conditions.[29] Therefore, although the leaky Cre activity led to *p38α/β* deletion prior to antigenic stimulation, the functional phenotypes observed are likely due to effective *p38α/β* ablation in naïve CD8$^+$ T cells. However, residual expression in some cells cannot be completely excluded, and early deletion kinetics should be interpreted cautiously. Despite this early deletion, only minor effects on peripheral T-cell development were detected, which contrasts with earlier reports suggesting a critical role for thymic p38 signaling in CD8$^+$ T-cell maturation.[16,17] While the differences in experimental conditions could contribute to this discrepancy, our RNA-seq

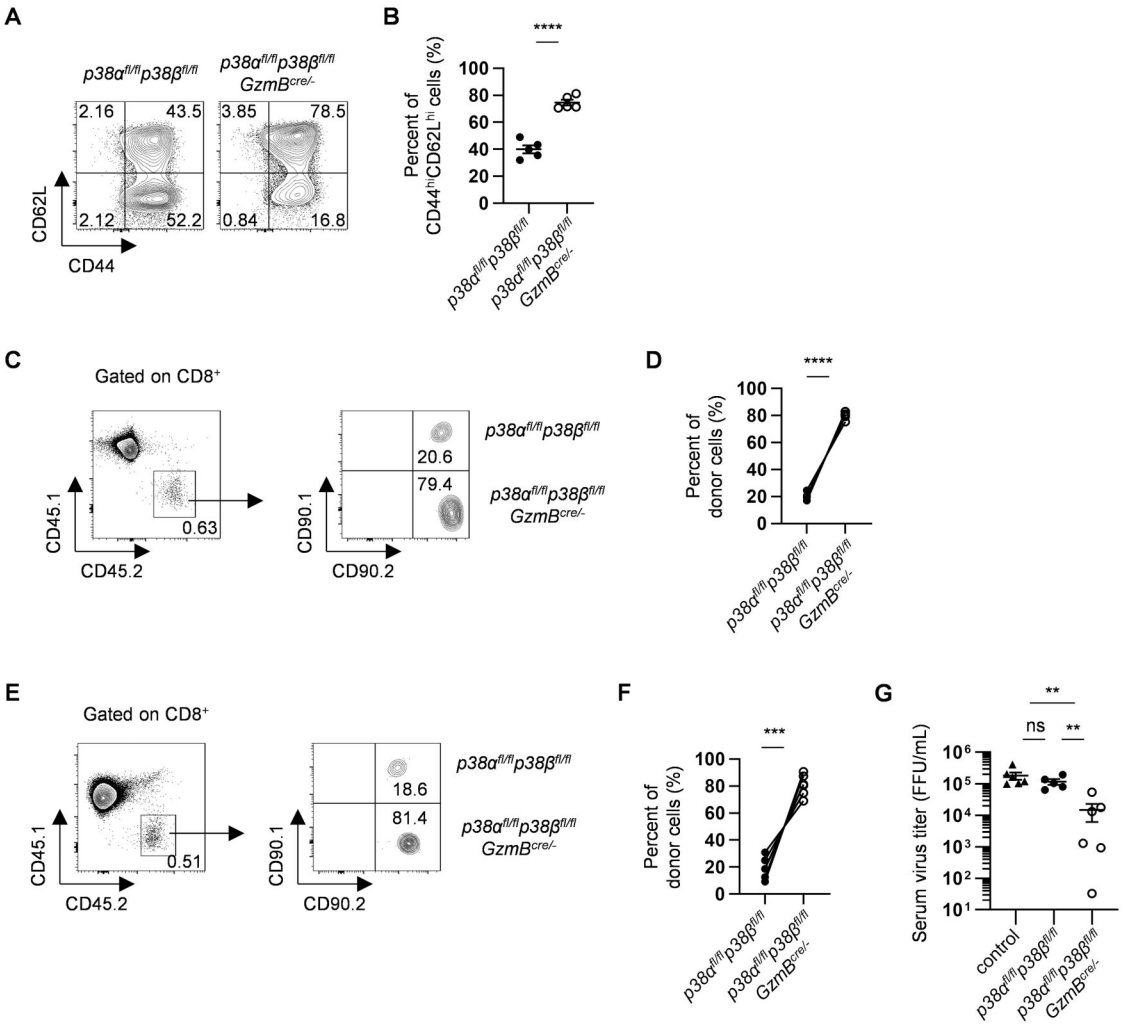

Figure 8. *p38α/β* deletion improves persistence and protective effect of in vitro differentiated $CD8^+$ T cells during adoptive transfer. (A and B) CD44 and CD62L expression on in vitro differentiated $p38\alpha^{fl/fl}p38\beta^{fl/fl}$ and $p38\alpha^{fl/fl}p38\beta^{fl/fl}GzmB^{cre/-}$ P14 T cells (A). Percentages of $CD44^{hi}CD62L^{hi}$ cells were calculated ($n = 5$) (B). (C–F) In vitro differentiated $p38\alpha^{fl/fl}p38\beta^{fl/fl}$ (*CD90.1/CD90.2*) and $p38\alpha^{fl/fl}p38\beta^{fl/fl}GzmB^{cre/-}$ (*CD90.2/CD90.2*) CD45.2 P14 T cells were equally co-transferred to CD45.1 mice; donor cells were gated on splenic $CD8^+$ T cells the following day before infection (C) or 7 days post–$LCMV_{Arm}$ infection (E). Percentages of donor cells before (D) and after (F) infection were calculated ($n = 6$). (G) Serum $LCMV_{Cl13}$ titers of control and P14 T cell–bearing mice were determined at day 10 postinfection ($n = 5$ to 6). Values are presented as mean ± SEM. Data are representative of 2 or 3 independent experiments. Statistical analyses were performed with unpaired Student *t*-test. $^{**}P < 0.01$, $^{***}P < 0.001$, $^{****}P < 0.0001$; ns, not significant. FFU, focus-forming unit.

analysis showed only limited transcriptional perturbations by *p38α/β* deletion in naïve $CD8^+$ T cells (Fig. S2A–C). Moreover, we minimized potential confounding effects of thymic *p38α/β* loss by confirming phenotypic similarities in naïve $CD8^+$ T cells between genotypes, and by employing adoptive co-transfer strategies to dissect cell-intrinsic roles of p38 signaling in $CD8^+$ T-cell fate determination (Fig. 7 and Figs. S1, S2, and S9). Intriguingly, depletion of *p38α/β* did not impact the total numbers of effector or memory cells but instead promoted the formation of MPECs and central memory $CD8^+$ T cells following acute $LCMV_{Arm}$ infection (Figs. 1D–F, 5B–D). This is not often the case as most genes reported to act on CTL differentiation also affect expansion at the same time, resulting in an unsatisfactory long-term immune response.[21,32]

In previous studies, anti-CD3 and anti-CD28 stimulation was generally utilized to activate TCR signaling in vitro, and sustained p38 kinase activity was observed in this context.[49] However, we did not anticipate that even the protein level of p38 would be responsively regulated in our in vivo study of p38 activation during the antigen-specific $CD8^+$ T-cell response (Fig. 1A, B). Additionally, in vitro culture using anti-CD3 and anti-CD28 stimulation yielded more cells due to decreased cell death in the population with p38 signaling blockade.[21] In contrast, our in vivo immunization results and in vitro expansion scheme using peptide and IL-2 did not exhibit increased $CD8^+$ T-cell expansion or survival in the absence of *p38α/β* (Fig. 1D and Figs. S3B, S10A, B). Moreover, the importance of p38 in T-cell functionality differs between endogenous and in vitro differentiated CTLs. Interestingly, in the endogenous response, although *p38α/β* deficiency attenuated cytokine expression levels in both $GP_{33–41}$ and $NP_{396–404}$ peptide–responsive $CD8^+$ T cells, impaired in vivo cytotoxicity was mainly evident in $GP_{33–41}$-specific cells (Fig. 3B–D). This suggests that p38 signaling may differentially modulate effector functions depending on epitope specificity, potentially reflecting variations in TCR affinity, peptide-MHC stability, or co-stimulatory signals. After

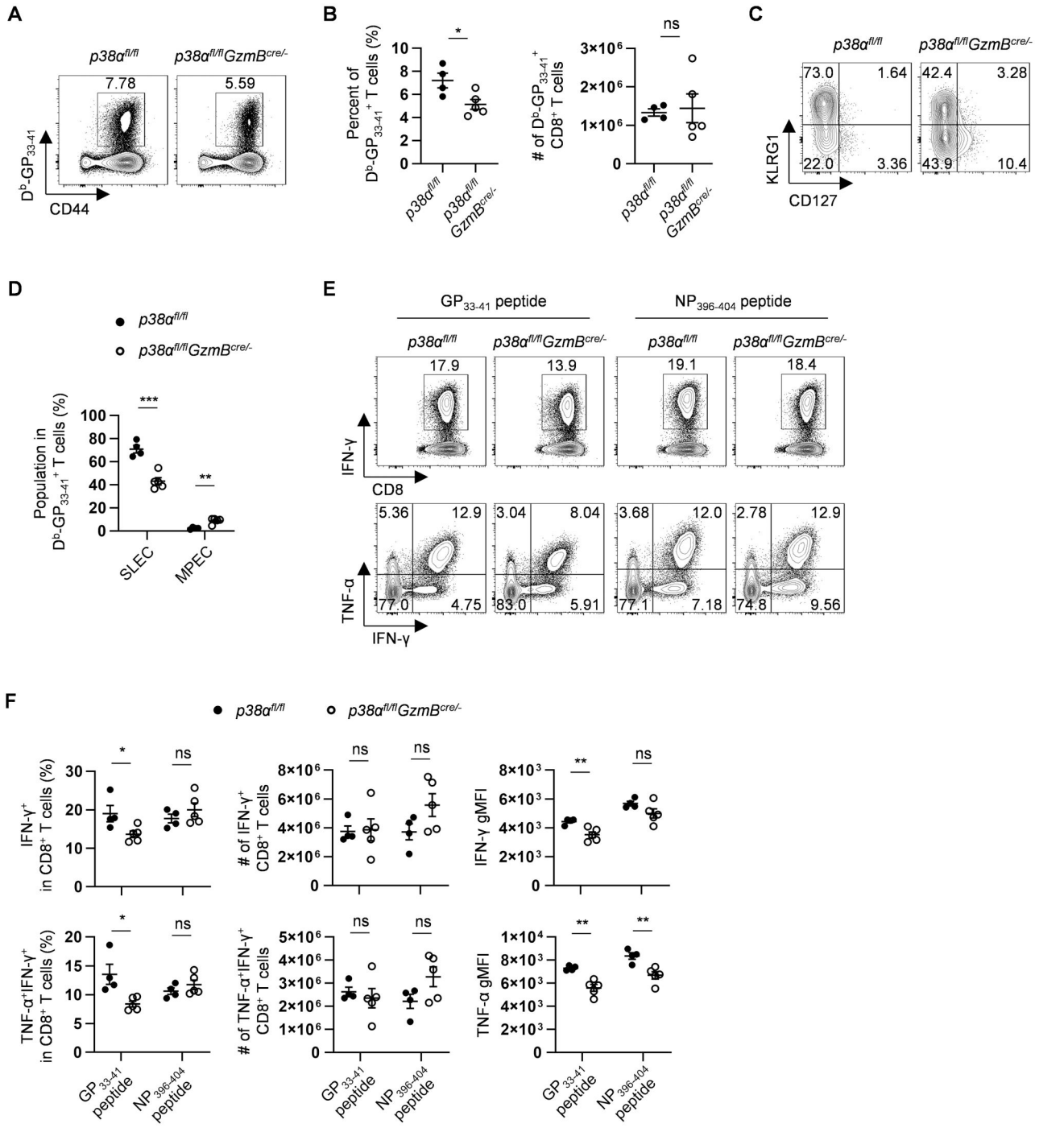

Figure 9. p38α predominates in promoting CD8$^+$ T-cell terminal differentiation. (A and B) Representative plots of splenic CD44$^+$D^b-GP$_{33-41}$-tetramer$^+$ cells in CD8$^+$ T cells from *p38α$^{fl/fl}$* and *p38α$^{fl/fl}$GzmB$^{cre/-}$* mice 8 days after LCMV$_{Arm}$ infection (A). Splenic D^b-GP$_{33-41}$-tetramer$^+$ CD8$^+$ T-cell percentages and numbers ($n = 4$ to 5) (B). (C and D) Expression of KLRG1 and CD127 on splenic D^b-GP$_{33-41}$-tetramer$^+$ CD8$^+$ T cells at day 8 post–LCMV$_{Arm}$ infection (C). Percentages of KLRG1^{hi}CD127^{lo} (SLEC) and KLRG1^{lo}CD127^{hi} (MPEC) populations in D^b-GP$_{33-41}$-tetramer$^+$ CD8$^+$ T cells ($n = 4$ to 5) (D). (E and F) Splenocytes were intracellularly stained for IFN-γ and TNF-α production after in vitro peptide stimulation, with plots gated on CD8$^+$ T cells (E). Frequencies and numbers of splenic IFN-γ$^+$ CD8$^+$ T cells, IFN-γ gMFI, percentages and numbers of TNF-α and IFN-γ–co-producing CD8$^+$ T cells, and TNF-α gMFI were calculated ($n = 4$ to 5) (F). Values are represented as mean ± SEM. Data are representative of 2 independent experiments. Statistical analyses were performed with unpaired Student *t*-test. $^*P < 0.05$, $^{**}P < 0.01$, $^{***}P < 0.001$; ns, not significant.

in vitro differentiation, *p38α/β* deletion enabled IFN-γ expression, although the acquisition of TNF-α expression remained impaired (Fig. S10D). Our data corresponded to the finding that p38 inhibition increased IFN-γ–producing but mildly reduced TNF-α–producing cell proportions in expanded mouse CD8$^+$ T cells in vitro.[21] As in the in vitro differentiated CD8$^+$ T cells, p38 inhibition impacts reactive oxygen species levels and glucose consumption through regulating multiple metabolism pathways, and the RNA-seq results showed gene set enrichment on DNA damage and the mechanistic target of rapamycin (mTOR) pathways.[21] However, this was not observed in our RNA-seq results of CD8$^+$ T cells in vivo upon viral infection (Fig. 4B). The differential requirement of p38 signaling in inflammatory

cytokine expression in different educated CD8$^+$ T cells warrants further investigation.

Indeed, the promotion of SLEC generation by p38 signaling echoes our prior research demonstrating that p38 signaling in B cells governs plasma cell differentiation without affecting germinal center B-cell proliferation.[25] Together, our results suggest that p38 signaling in lymphocytes plays a crucial role in driving effector cell terminal differentiation while exerting limited influence on cell proliferation. However, it remains an important issue to determine how p38 signaling regulates CD8$^+$ T-cell differentiation. BLIMP1, a key transcription factor downstream of the p38 pathway in plasma cell differentiation,[25] displayed a similar function in repressing central memory CD8$^+$ T-cell formation like p38.[50] However, the mRNA level of *Blimp-1* was not altered by *p38* deficiency according to our RNA-seq data, unlike what was observed in plasma cell differentiation. The transcriptional repressor *Zeb2* was downregulated in *p38*-deficient CD8$^+$ T cells, which has been reported to promote SLEC differentiation as well.[32] Whether there exists a possible p38-ZEB2 axis as an unappreciated approach that regulates effector T-cell differentiation needs to be further explored. A noticeable alteration on gene expressions triggered by *p38* deficiency is the sets of surface receptors (Fig. 4B), and how these changes will influence CD8$^+$ T-cell chemotaxis, exhaustion, activity regulation, etc, needs to be plumbed. Overall, how the transcriptional programs of effector and memory CD8$^+$ T cells were targeted by p38 is worth further investigation.

The induction of IL-2 production through p38 signaling abrogation is proved to be cell-intrinsic (Fig. 7G, H), but the underlying mechanism by which this pathway targets *Il-2* expression regulation requires further investigation. Apart from the memory cells, another consideration is whether this mechanism controlling *Il-2* expression is still stationary in CD8$^+$ T cells arising from chronic infection. In an earlier report, CD8$^+$ T cells from transgenic mice with dominant negative DUSP16 expression produced an increased amount of IL-2 by raising JNK phosphorylation level, as JNK1 activity can promote IL-2 production and can be dampened by the MAPK phosphatase DUSP16.[51] Taking the elevated transcriptional level of *Dusp16* in *p38*-dificient cells into account, JNK signaling seemed to be balanced whether in the presence or absence of p38 in CD8$^+$ T cells. Taking account of the immune regulatory receptors regulated by p38 signaling, we wonder if p38 could be an immune checkpoint protein to deactivate. Hence, it would be meaningful to explore the effect of p38 signaling restraining in memory and exhausted CD8$^+$ T cells, as many peripheral T cells have already experienced the effector phase after activation in WT individuals.

Memory cells are critical for the efficacy of vaccines and long-term therapeutic outcomes in adoptive cell therapy.[47] Recent studies have shown that pharmacological inhibition of p38 signaling during adoptive transfer enhances the secondary expansion of CD8$^+$ T cells, leading to improved outcomes in tumor cell therapy.[21,22] Given the observation that genetic deletion of *p38α/β* augmented central memory CD8$^+$ T-cell generation and recall response, the in vitro differentiated T cells lacking p38 signaling exhibited better persistence and control of chronic LCMV infection in our study (Fig. 8C, D, G). Our in vivo cytotoxicity assays revealed that despite reduced per-cell killing capacity, the overall protective efficacy of *p38α/β*-deficient memory CD8$^+$ T cells was maintained or even enhanced, likely due to increased cell numbers compensating for impaired effector function at the single-cell level (Fig. 6C, D and Fig. S8C). Interestingly, our adoptive transfer experiments demonstrated that *p38α/β*-deficient memory CD8$^+$ T cells did not exhibit increased secondary expansion compared to WT counterparts (Fig. 8C–F), indicating that the improved recall response could also be driven by better memory cell maintenance rather than a proliferative advantage. Furthermore, our analysis of single-gene knockout data indicates that p38α alone is sufficient to promote the generation of short-lived effector cells (Fig. 9C, D), although p38β owns a compensative function to p38α in many cases, possibly due to the dozens of times lower level of *p38β* expression than *p38α* expression in CD8$^+$ T cells indicated by RNA-seq data.

In summary, our study elucidates a cell-intrinsic role of p38α/β as a molecular switch that biases MPEC formation toward SLEC differentiation. Additionally, depletion of *p38α/β* enhances central memory T-cell formation, thereby bolstering a stronger secondary response. The orchestrated transcriptional program by the p38 pathway primarily influences effector and memory T-cell differentiation. Consequently, our findings suggest that disrupting p38 signaling may offer an advanced strategy to enhance the protective function of adoptive T-cell immunotherapies or vaccines against infections and tumors.

Author contributions

Conceptualization: L.H., J.H., J.W. Methodology: L.H., H. L., Y.F., D.L., L.Z., Z.W., Y.C., W.L. Investigation: L.H., H. L., Y.F., D.L., L.Z., Z.W., Y.C., W.L. Data curation: L.H., L. Z. (CyTOF), Z.W. (RNA-seq). Formal analysis: L.H., L.Z., Z.W. Visualization: L.H., L.Z., Z.W. Writing—original draft: L.H., J.W. Writing—review & editing: G.F., N.X., J. H., J.W. Supervision: J.H., J.W. Project administration: J.H., J.W. Funding acquisition: J.H., J.W.

Supplementary material

Supplementary material is available at *The Journal of Immunology* online.

Funding

This work was supported by the National Natural Science Foundation of China (82388201 to J.H.), the National Key Research and Development Program of China (2020YFA0803500 to J.H., 2020YFA0803501 to J.W.), the Chinese Academy of Medical Sciences (CAMS) Innovation Fund for Medical Sciences (2019-I2M-5-062 to J.H.), the Fujian Province Central to Local Science and Technology Development Special Program (2022L3079 to J.H.), the Fu-Xia-Quan Zi-Chuang District Cooperation Program (3502ZCQXT2022003 to J.H.), and the Xiamen Natural Science Foundation Project (3502Z202373004 to J.W.).

Conflicts of interest

None declared.

Data availability

The RNA-seq data generated in this study have been deposited in the Gene Expression Omnibus under accession codes GSE298331 and GSE239348.

References

1. Turner SJ, Bennett TJ, La Gruta NL. CD8(+) T-cell memory: the why, the when, and the how. Cold Spring Harb Perspect Biol. 2021;13:13.
2. Mittrucker HW, Visekruna A, Huber M. Heterogeneity in the differentiation and function of CD8(+) T cells. Arch Immunol Ther Exp (Warsz). 2014;62:449–458.
3. Halle S, Halle O, Forster R. Mechanisms and dynamics of T cell-mediated cytotoxicity in vivo. Trends Immunol. 2017;38:432–443.
4. Kaech SM, Cui W. Transcriptional control of effector and memory CD8+ T cell differentiation. Nat Rev Immunol. 2012; 12:749–761.
5. Samji T, Khanna KM. Understanding memory CD8(+) T cells. Immunol Lett. 2017;185:32–39.
6. Joshi NS et al. Inflammation directs memory precursor and short-lived effector CD8(+) T cell fates via the graded expression of T-bet transcription factor. Immunity. 2007;27:281–295.
7. Muroyama Y, Wherry EJ. Memory T-cell heterogeneity and terminology. Cold Spring Harb Perspect Biol. 2021;13:a037929.
8. Martin MD, Badovinac VP. Defining memory CD8 T cell. Front Immunol. 2018;9:2692.
9. Toumi R et al. Autocrine and paracrine IL-2 signals collaborate to regulate distinct phases of CD8 T cell memory. Cell Rep. 2022; 39:110632.
10. Feau S, Arens R, Togher S, Schoenberger SP. Autocrine IL-2 is required for secondary population expansion of CD8(+) memory T cells. Nat Immunol. 2011;12:908–913.
11. Canovas B, Nebreda AR. Diversity and versatility of p38 kinase signalling in health and disease. Nat Rev Mol Cell Biol. 2021; 22:346–366.
12. Jirmanova L, Giardino Torchia ML, Sarma ND, Mittelstadt PR, Ashwell JD. Lack of the T cell-specific alternative p38 activation pathway reduces autoimmunity and inflammation. Blood. 2011; 118:3280–3289.
13. Salvador JM, Jr., et al. Alternative p38 activation pathway mediated by T cell receptor-proximal tyrosine kinases. Nat Immunol. 2005;6:390–395.
14. Jirmanova L, Sarma DN, Jankovic D, Mittelstadt PR, Ashwell JD. Genetic disruption of p38alpha Tyr323 phosphorylation prevents T-cell receptor–mediated p38alpha activation and impairs interferon-gamma production. Blood. 2009;113:2229–2237.
15. Cook R, Wu CC, Kang YJ, Han J. The role of the p38 pathway in adaptive immunity. Cell Mol Immunol. 2007;4:253–259.
16. Hayakawa M et al. Loss of functionally redundant p38 isoforms in T cells enhances regulatory T cell induction. J Biol Chem. 2017; 292:1762–1772.
17. Ritprajak P, Hayakawa M, Sano Y, Otsu K, Park JM. Cell type-specific targeting dissociates the therapeutic from the adverse effects of protein kinase inhibition in allergic skin disease. Proc Natl Acad Sci U S A. 2012;109:9089–9094.
18. Risco A, Martin-Serrano MA, Barber DF, Cuenda A. p38gamma and p38delta are involved in T lymphocyte development. Front Immunol. 2018;9:65.
19. Meng D et al. p38alpha deficiency in T cells ameliorates diet-induced obesity, insulin resistance, and adipose tissue senescence. Diabetes. 2022;71:1205–1217.
20. Salvador-Bernaldez M et al. p38alpha regulates cytokine-induced IFNgamma secretion via the Mnk1/eIF4E pathway in Th1 cells. Immunol Cell Biol. 2017;95:814–823.
21. Gurusamy D et al. Multi-phenotype CRISPR-Cas9 screen identifies p38 kinase as a target for adoptive immunotherapies. Cancer Cell. 2020;37:818–833.e9.
22. Chen S et al. p38 inhibition enhances TCR-T cell function and antagonizes the immunosuppressive activity of TGF-beta. Int Immunopharmacol. 2021;98:107848.
23. Jacob J, Baltimore D. Modelling T-cell memory by genetic marking of memory T cells in vivo. Nature. 1999;399:593–597.
24. Zhou X, Ramachandran S, Mann M, Popkin DL. Role of lymphocytic choriomeningitis virus (LCMV) in understanding viral immunology: past, present and future. Viruses. 2012;4:2650–2669.
25. Wu J et al. A p38alpha-BLIMP1 signalling pathway is essential for plasma cell differentiation. Nat Commun. 2022;13:7321.
26. Tang J et al. Themis suppresses the effector function of CD8(+) T cells in acute viral infection. Cell Mol Immunol. 2023; 20:512–524.
27. Kim MV, Ouyang W, Liao W, Zhang MQ, Li MO. The transcription factor Foxo1 controls central-memory CD8+ T cell responses to infection. Immunity. 2013;39:286–297.
28. Hauser C, Zipprich F, Leblond I, Wirth S, Hügin AW. Protective immunity from naive CD8+ T cells activated in vitro with MHC class I binding immunogenic peptides and IL-2 in the absence of specialized APCs. J Immunol. 1999;163:330–336.
29. Xu Y, Evaristo C, Alegre ML, Gurbuxani S, Kee BL. Analysis of GzmbCre as a model system for gene deletion in the natural killer cell lineage. PLoS One. 2015;10:e0125211.
30. Herndler-Brandstetter D et al. KLRG1+ effector CD8+ T cells lose KLRG1, differentiate into all memory T cell lineages, and convey enhanced protective immunity. Immunity. 2018;48: 716–729.e8.
31. Li O, Zheng P, Liu Y. CD24 expression on T cells is required for optimal T cell proliferation in lymphopenic host. J Exp Med. 2004;200:1083–1089.
32. Omilusik KD et al. Transcriptional repressor ZEB2 promotes terminal differentiation of CD8+ effector and memory T cell populations during infection. J Exp Med. 2015;212:2027–2039.
33. Kaech SM et al. Selective expression of the interleukin 7 receptor identifies effector CD8 T cells that give rise to long-lived memory cells. Nat Immunol. 2003;4:1191–1198.
34. Dong H, Buckner A, Prince J, Bullock T. Frontline science: late CD27 stimulation promotes IL-7Ralpha transcriptional re-expression and memory T cell qualities in effector CD8(+) T cells. J Leukoc Biol. 2019;106:1007–1019.
35. Bachmann MF, Wolint P, Schwarz K, Jäger P, Oxenius A. Functional properties and lineage relationship of CD8+ T cell subsets identified by expression of IL-7 receptor alpha and CD62L. J Immunol. 2005;175:4686–4696.
36. Hu JK, Kagari T, Clingan JM, Matloubian M. Expression of chemokine receptor CXCR3 on T cells affects the balance between effector and memory CD8 T-cell generation. Proc Natl Acad Sci U S A. 2011;108:E118–E127.
37. Hwang JY, Sun Y, Carroll CR, Usherwood EJ. Neuropilin-1 regulates the secondary CD8 T cell response to virus infection. mSphere. 2019;4:e00221–19.
38. Liu N et al. Serine protease inhibitor 2A is a protective factor for memory T cell development. Nat Immunol. 2004;5:919–926.
39. Evrard M et al. Sphingosine 1-phosphate receptor 5 (S1PR5) regulates the peripheral retention of tissue-resident lymphocytes. J Exp Med. 2022;219:e20210116.
40. McGraw JM et al. JAML promotes CD8 and gammadelta T cell antitumor immunity and is a novel target for cancer immunotherapy. J Exp Med. 2021;218:e20202644.
41. Wang B et al. Combination cancer immunotherapy targeting PD-1 and GITR can rescue CD8(+) T cell dysfunction and maintain memory phenotype. Sci Immunol. 2018;3:eaat7061.
42. Hajaj E et al. SLAMF6 deficiency augments tumor killing and skews toward an effector phenotype revealing it as a novel T cell checkpoint. Elife. 2020;9:e52539.
43. Workman CJ et al. Lymphocyte activation gene-3 (CD223) regulates the size of the expanding T cell population following antigen activation in vivo. J Immunol. 2004;172:5450–5455.

44. Pedicord VA, Montalvo W, Leiner IM, Allison JP. Single dose of anti-CTLA-4 enhances CD8+ T-cell memory formation, function, and maintenance. Proc Natl Acad Sci U S A. 2011;108:266–271.
45. Laurie SJ et al. 2B4 mediates inhibition of CD8(+) T cell responses via attenuation of glycolysis and cell division. J Immunol. 2018; 201:1536–1548.
46. Roberts AD, Ely KH, Woodland DL. Differential contributions of central and effector memory T cells to recall responses. J Exp Med. 2005;202:123–133.
47. Liu Q, Sun Z, Chen L. Memory T cells: strategies for optimizing tumor immunotherapy. Protein Cell. 2020;11:549–564.
48. Han J, Wu J, Silke J. An overview of mammalian p38 mitogen-activated protein kinases, central regulators of cell stress and receptor signaling. F1000Res. 2020;9:F1000 Faculty Rev-653.
49. Tan H et al. Integrative proteomics and phosphoproteomics profiling reveals dynamic signaling networks and bioenergetics pathways underlying T cell activation. Immunity. 2017; 46:488–503.
50. Rutishauser RL et al. Transcriptional repressor Blimp-1 promotes CD8(+) T cell terminal differentiation and represses the acquisition of central memory T cell properties. Immunity. 2009; 31:296–308.
51. Kumabe S et al. Dual specificity phosphatase16 is a negative regulator of c-Jun NH2-terminal kinase activity in T cells. Microbiol Immunol. 2010;54:105–111.

The Journal of Immunology, 2025, 00, 1–17
https://doi.org/10.1093/jimmun/vkaf214
Research Article